

- [14] Fukuda K, Izumo S. Angiotensin II potentiates DNA synthesis in AT-1 transformed cardiomyocytes. *J Mol Cell Cardiol* 1998;30:2069–80.
- [15] Myer A, Olson EN, Klein WH. MyoD cannot compensate for the absence of myogenin during skeletal muscle differentiation in murine embryonic stem cells. *Dev Biol* 2001;229:340–50.
- [16] Yamada H, Akishita M, Ito M, Tamura K, Daviet L, Lehtonen JY, et al. AT2 receptor and vascular smooth muscle cell differentiation in vascular development. *Hypertension* 1999;33:1414–9.
- [17] Jackson KA, Snyder DS, Goodell MA. Skeletal muscle fiber-specific green autofluorescence: potential for stem cell engraftment artifacts. *Stem Cells* 2004;22:180–7.
- [18] Tomita S, Li RK, Weisel RD, Mickle DA, Kim EJ, Sakai T, et al. Autologous transplantation of bone marrow cells improves damaged heart function. *Circulation* 1999;100(Suppl. 19):II247.
- [19] Jackson KA, Majka SM, Wang H, Pocius J, Hartley CJ, Majesky MW, et al. Regeneration of ischemic cardiac muscle and vascular endothelium by adult stem cells. *J Clin Invest* 2001;107:1395–402.
- [20] Condorelli G, Borello U, De Angelis L, Latronico M, Sirabella D, Coletta M, et al. Cardiomyocytes induce endothelial cells to transdifferentiate into cardiac muscle: Implications for myocardium regeneration. *Proc Natl Acad Sci U S A* 2001;98:10733–8.
- [21] Sachinidis A, Fleischmann BK, Kolossov E, Wartenberg M, Sauer H, Hescheler J. Cardiac specific differentiation of mouse embryonic stem cells. *Cardiovasc Res* 2003;58:278–91.
- [22] Zweigerdt R, Burg M, Willbold E, Abts H, Ruediger M. Generation of confluent cardiomyocyte monolayers derived from embryonic stem cells in suspension: a cell source for new therapies and screening strategies. *Cytotherapy* 2003;5:399–413.
- [23] Zandstra PW, Bauwens C, Yin T, Liu Q, Schiller H, Zweigerdt R, et al. Scalable production of embryonic stem cell-derived cardiomyocytes. *Tissue Eng* 2003;9:767–78.
- [24] Moore JC, Spijker R, Martens AC, de Boer T, Rook MB, van der Heyden MA, et al. A P19C16 EGFP reporter line to quantify cardiomyocyte differentiation of stem cells. *Int J Dev Biol* 2004;48:47–55.
- [25] Kolossov E, Fleischmann BK, Liu Q, Bloch W, Viatchenko-Karpinski S, Manzke O, et al. Functional characteristics of ES cell-derived cardiac precursor cells identified by tissue-specific expression of the green fluorescent protein. *J Cell Biol* 1998;143:2045–56.
- [26] Reinecke H, Murry CE. Taking the death toll after cardiomyocyte grafting: a reminder of the importance of quantitative biology. *J Mol Cell Cardiol* 2002;34:251–3.
- [27] Zhang M, Methot D, Poppa V, Fujio Y, Walsh K, Murry CE. Cardiomyocyte grafting for cardiac repair: graft cell death and anti-death strategies. *J Mol Cell Cardiol* 2001;33:907–21.
- [28] Takeda Y, Mori T, Imabayashi H, Kiyono T, Gojo S, Miyoshi S, et al. Can the life span of human marrow stromal cells be prolonged by bmi-1, E6, E7, and/or telomerase without affecting cardiomyogenic differentiation? *J Gene Med* 2004;6:833–45.

Transplantation of Mesenchymal Stem Cells Improves Cardiac Function in a Rat Model of Dilated Cardiomyopathy

Noritoshi Nagaya, MD; Kenji Kangawa, PhD; Takefumi Itoh, MD; Takashi Iwase, MD; Shinsuke Murakami, MD; Yoshinori Miyahara, MD; Takafumi Fujii, MD; Masaaki Uematsu, MD; Hajime Ohgushi, MD; Masakazu Yamagishi, MD; Takeshi Tokudome, MD; Hidezo Mori, MD; Kunio Miyatake, MD; Soichiro Kitamura, MD

Background—Pluripotent mesenchymal stem cells (MSCs) differentiate into a variety of cells, including cardiomyocytes and vascular endothelial cells. However, little information is available about the therapeutic potency of MSC transplantation in cases of dilated cardiomyopathy (DCM), an important cause of heart failure.

Methods and Results—We investigated whether transplanted MSCs induce myogenesis and angiogenesis and improve cardiac function in a rat model of DCM. MSCs were isolated from bone marrow aspirates of isogenic adult rats and expanded *ex vivo*. Cultured MSCs secreted large amounts of the angiogenic, antiapoptotic, and mitogenic factors vascular endothelial growth factor, hepatocyte growth factor, adrenomedullin, and insulin-like growth factor-1. Five weeks after immunization, MSCs or vehicle was injected into the myocardium. Some engrafted MSCs were positive for the cardiac markers desmin, cardiac troponin T, and connexin-43, whereas others formed vascular structures and were positive for von Willebrand factor or smooth muscle actin. Compared with vehicle injection, MSC transplantation significantly increased capillary density and decreased the collagen volume fraction in the myocardium, resulting in decreased left ventricular end-diastolic pressure (11 ± 1 versus 16 ± 1 mm Hg, $P < 0.05$) and increased left ventricular maximum dP/dt (6767 ± 323 versus 5138 ± 280 mm Hg/s, $P < 0.05$).

Conclusions—MSC transplantation improved cardiac function in a rat model of DCM, possibly through induction of myogenesis and angiogenesis, as well as by inhibition of myocardial fibrosis. The beneficial effects of MSCs might be mediated not only by their differentiation into cardiomyocytes and vascular cells but also by their ability to supply large amounts of angiogenic, antiapoptotic, and mitogenic factors. (*Circulation*. 2005;112:1128-1135.)

Key Words: myocytes ■ angiogenesis ■ heart failure ■ growth substances ■ transplantation

Despite advances in medical and surgical procedures, congestive heart failure remains a leading cause of cardiovascular morbidity and mortality.¹ Idiopathic dilated cardiomyopathy (DCM), a primary myocardial disease of unknown etiology characterized by a loss of cardiomyocytes and an increase in fibroblasts, is an important cause of heart failure.² Although myocyte mitosis and the presence of cardiac precursor cells in adult hearts have recently been reported,³ the death of large numbers of cardiomyocytes results in the development of heart failure. Thus, restoring lost myocardium would be desirable for the treatment of DCM.

Mesenchymal stem cells (MSCs) are pluripotent, adult stem cells residing within the bone marrow microenviron-

ment.⁴ In contrast to their hematopoietic counterparts, MSCs are adherent and can be expanded in culture. MSCs can differentiate not only into osteoblasts, chondrocytes, neurons, and skeletal muscle cells but also into vascular endothelial cells⁵ and cardiomyocytes.^{6,7} In vitro, MSCs can be induced to differentiate into beating cardiomyocytes by 5-azacytidine treatment.⁸ In vivo, MSCs directly injected into an infarcted heart have been shown to induce myocardial regeneration and improve cardiac function.⁹ In addition, MSC implantation induces therapeutic angiogenesis in a rat model of hindlimb ischemia through vascular endothelial growth factor (VEGF) production by MSCs.^{10,11} Myocardial blood flow abnormalities, even in the presence of angiographically normal coronary arteries, have been documented in patients with DCM.¹²

Received August 18, 2004; revision received April 28, 2005; accepted May 10, 2005.

From the Departments of Regenerative Medicine and Tissue Engineering (N.N., T.I., T.I., S.M.), Internal Medicine (N.N., M.Y., K.M.), Biochemistry (K.K., T.T.), and Cardiac Physiology (Y.M., T.F., H.M.), National Cardiovascular Center Research Institute, Osaka; the Cardiovascular Division (M.U.), Kansai Rosai Hospital, Hyogo; the Tissue Engineering Research Center (H.O.), National Institute of Advanced Industrial Science and Technology, Hyogo; and the Department of Cardiovascular Surgery (S.K.), National Cardiovascular Center, Osaka, Japan.

Reprint requests to Noritoshi Nagaya, MD, Department of Regenerative Medicine and Tissue Engineering, National Cardiovascular Center Research Institute, 5-7-1 Fujishirodai, Suita, Osaka 565-8565, Japan. E-mail nnagaya@ri.ncvc.go.jp

© 2005 American Heart Association, Inc.

Circulation is available at <http://www.circulationaha.org>

DOI: 10.1161/CIRCULATIONAHA.104.500447

These findings raise the possibility that transplanted MSCs have beneficial effects on myocardial structure and function via myogenesis and angiogenesis. However, little information is available about the therapeutic potential of MSCs for DCM.

A unique model of myocarditis in the rat has been created by immunization with porcine cardiac myosin,¹³ which results in severe heart failure characterized by increased cardiac fibrosis and left ventricular (LV) dilation.¹⁴ Thus, the late phase of this model can serve as a model of DCM.

The purpose of this study was to investigate the following topics: (1) whether transplantation of MSCs induces myogenesis and angiogenesis, decreases collagen deposition in the myocardium, and thereby improves cardiac function in a rat model of DCM and (2) whether the beneficial effects of MSCs are mediated by their differentiation into cardiomyocytes and vascular cells and/or by their supplying angiogenic, antiapoptotic, and mitogenic factors.

Methods

Expansion of Bone Marrow MSCs

MSC expansion was performed according to previously described methods.⁴ In brief, we humanely killed male Lewis rats and harvested bone marrow by flushing their femoral and tibial cavities with phosphate-buffered saline (PBS). Bone marrow cells were cultured in α -minimal essential medium supplemented with 10% fetal bovine serum and antibiotics. A small number of cells developed visible symmetric colonies by days 5 to 7. Nonadherent hematopoietic cells were removed, and the medium was replaced. The adherent, spindle-shaped MSC population expanded to $>5 \times 10^7$ cells within ≈ 4 to 5 passages after the cells were first plated.

Flow Cytometry

Cultured MSCs were analyzed by fluorescence-activated cell sorting (FACS) (FACScan flow cytometer, Becton Dickinson). Cells were incubated with fluorescein isothiocyanate (FITC)-conjugated mouse monoclonal antibodies against rat CD31 (clone TLD-3A12, Becton Dickinson), CD34 (clone ICO-115, Santa Cruz), CD45 (clone OX-1, Becton Dickinson), CD90 (clone OX-7, Becton Dickinson), vimentin (clone V9, Dako), and smooth muscle actin (SMA; clone IA4, Dako). FITC-conjugated hamster anti-rat CD29 monoclonal antibody (clone Ha2/5, Becton Dickinson) and rabbit anti-rat c-Kit polyclonal antibody (clone C-19, Santa Cruz) were used. Isotype-identical antibodies served as controls.

Model of DCM

Male Lewis rats weighing 220 to 250 g (Japan SLC Inc, Hamamatsu, Japan) were used in this study. These isogenic rats served as donors and recipients of MSCs to simulate autologous implantation. DCM was produced by inducing experimental myocarditis, as described previously.^{13,14} In brief, 1 mg (0.1 mL) of porcine heart myosin (Sigma) was mixed with an equal volume of Freund's complete adjuvant (Sigma) and injected into a footpad on days 1 and 7. Five weeks after immunization, these rats served as a model of heart failure due to DCM.

MSC Transplantation

In a preliminary experiment, we performed dose-response studies to obtain the maximal effects of cell transplantation. Because the effect of 10^6 MSCs was modest, we used 5×10^6 MSCs for transplantation. Five weeks after immunization, we injected a total of 5×10^6 MSCs/100 μ L PBS, or PBS alone, into the myocardium at 10 points. In brief, the LV was divided into 3 levels (basal, middle, and apical). The basal and middle levels were each subdivided into 4 segments, and the apical level was subdivided into 2 segments. Injection into

each segment was performed with a 27-gauge needle. Sham rats received intramyocardial injections of 100 μ L PBS. This protocol resulted in the creation of 3 groups: DCM rats given MSCs (MSC-treated DCM group, $n=10$); DCM rats given PBS (untreated DCM group, $n=10$); and sham rats given PBS (sham group, $n=10$). The Animal Care Committee of the National Cardiovascular Center approved this experimental protocol.

Echocardiographic Studies

Echocardiographic studies were performed by an investigator, blinded to treatment allocation, at 5 weeks after immunization (before treatment) and 4 weeks after cell transplantation (after treatment). Two-dimensional, targeted M-mode tracings were obtained at the level of the papillary muscles with an echocardiographic system equipped with a 7.5-MHz transducer (HP Sonos 5500, Hewlett-Packard).¹⁵ LV dimensions were measured according to the American Society for Echocardiology leading-edge method from at least 3 consecutive cardiac cycles. Fractional shortening was calculated as $(LVDd-LVds)/LVDd \times 100$, where $LVDd=LV$ diastolic dimension and $LVds=LV$ systolic dimension.

Hemodynamic Studies

Hemodynamic studies were performed 4 weeks after cell transplantation. A 1.5F micromanometer-tipped catheter (Millar Instruments) was inserted into the right carotid artery for measurement of mean arterial pressure.¹⁶ Next, the catheter was advanced into the LV for measurement of LV pressure. Hemodynamic variables were measured with a pressure transducer (model P23 ID, Gould) connected to a polygraph. After completion of these measurements, the left and right ventricles were excised and weighed.

Histological Examination

To detect fibrosis in cardiac muscle, the LV myocardium ($n=5$ from each group) was fixed in 10% formalin, cut transversely, embedded in paraffin, and stained with Masson's trichrome. Transverse sections were randomly obtained from the 3 levels (basal, middle, and apical), and 20 randomly selected fields per section ($n=60$ per animal) were analyzed. After each field was scanned and computerized with a digital image analyzer (WinRoof, Mitani Co), collagen volume fraction was calculated as the sum of all areas containing connective tissue divided by the total area of the image.¹⁵

To detect capillaries in the myocardium, samples of harvested muscle ($n=5$ each) were embedded in OCT compound (Miles Scientific), snap-frozen in LN_2 , cut into transverse sections, and stained for alkaline phosphatase by an indoxyltetrazolium method. Transverse sections were randomly obtained from the 3 levels (basal, middle, and apical), and 5 randomly selected fields per section ($n=15$ per animal) were analyzed. The number of capillaries was counted by light microscopy at a magnification of $\times 200$. The number of capillaries in each field was averaged and expressed as the number of capillary vessels. These morphometric studies were performed by 2 examiners who were blinded to treatment assignment.

Assessment of Cell Differentiation

Suspended MSCs were labeled with fluorescent dyes with use of a PKH26 red fluorescent cell linker kit (Sigma), as reported previously.¹⁷ Fluorescence-labeled MSCs were injected into the myocardium 5 weeks after immunization. Rats ($n=5$) were humanely killed 4 weeks after cell transplantation. LV samples were embedded in OCT compound, snap-frozen in LN_2 , and cut into sections. Immunofluorescence staining was performed with monoclonal mouse anti-cardiac troponin T (Novo), anti-desmin (Dako), anti-connexin-43 (Sigma), polyclonal rabbit anti-von Willebrand factor (Dako), and monoclonal mouse SMA (Dako). FITC-conjugated IgG antibody (BD Pharmingen) was used as a secondary antibody. To perform quantitative analysis of the magnitude of MSC differentiation into cardiomyocytes, heart cells from each rat ($n=5$) were isolated by incubation in balanced salt solution containing 0.06% collagenase type II (Worthington Biochemical Co), as reported previously.¹⁸ PKH26/troponin T double-positive cells were detected by FACS.

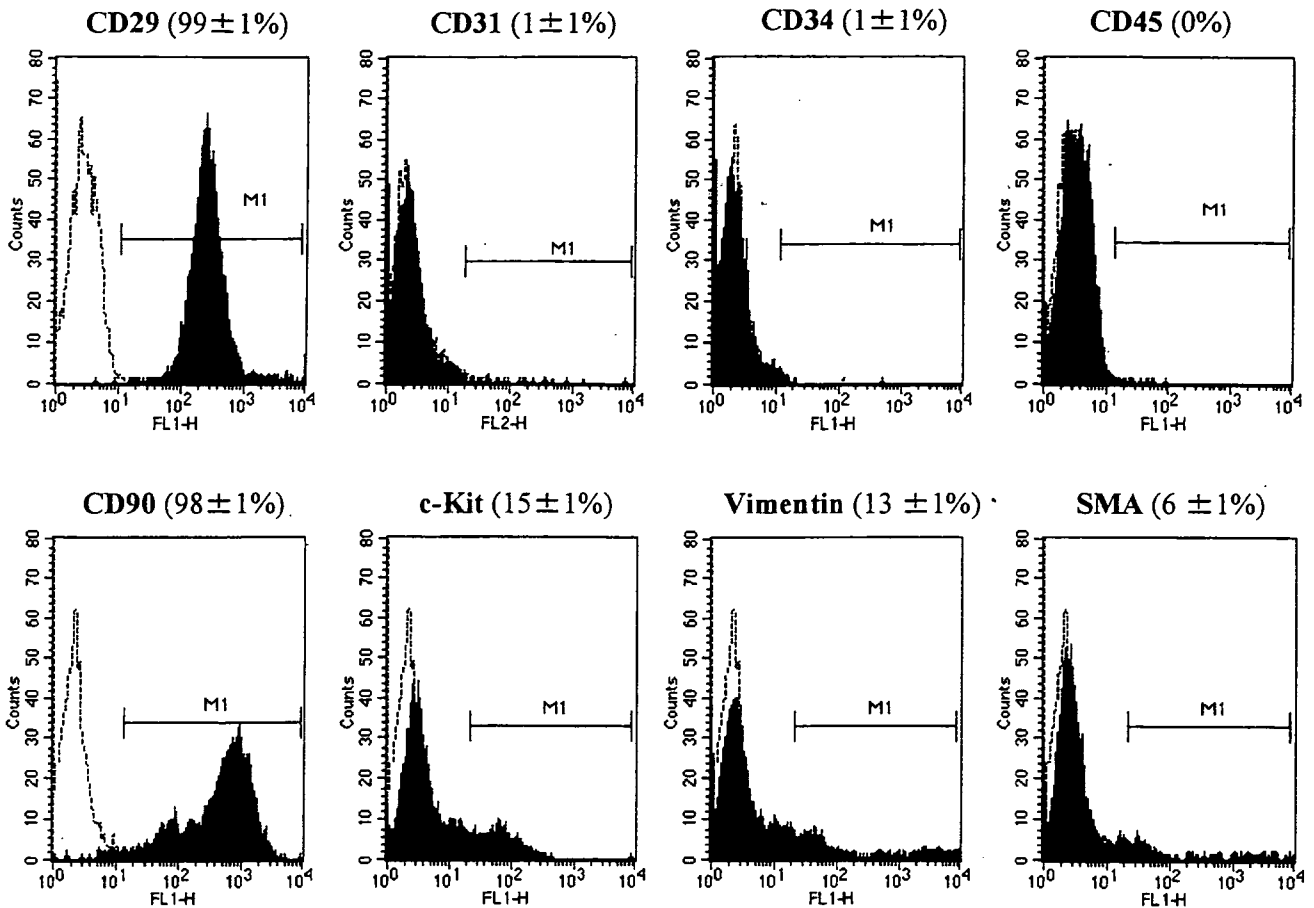


Figure 1. Flow-cytometric analysis of the adherent, spindle-shaped MSC population expanded to 4 to 5 passages. Most of the MSCs expressed CD29 and CD90, whereas they were negative for CD31, CD34, CD45, and SMA. Some of the cells were positive for c-Kit and vimentin.

Western Blot Analysis of Matrix Metalloproteinases

To identify the protein expression of matrix metalloproteinases (MMPs)-2 and -9, Western blotting was performed with rabbit polyclonal antibody raised against MMP-2 (Laboratory vision Co) and MMP-9 (Chemicon Co). The LV obtained from individual rats was used for comparison among the 3 groups ($n=5$ each). These samples were homogenized on ice in 0.1% Tween 20 homogenization buffer with a protease inhibitor. Then, 40 μg of protein was transferred into sample buffer, loaded on a 7.5% sodium dodecyl sulfate-polyacrylamide gel, and blotted onto a polyvinylidene fluoride membrane (Millipore Co). After being blocked for 120 minutes, the membrane was incubated with primary antibody at a dilution of 1:200. The membrane was incubated with peroxidase labeled with secondary antibody at a dilution of 1:1000. Positive protein bands were visualized with an ECL kit (Amersham) and measured by densitometry. Western blot analysis with a mouse polyclonal antibody raised against β -actin (Santa Cruz) was used as a protein loading control.

Assay for Angiogenic, Antiapoptotic, and Mitogenic Factors

To investigate whether MSCs produce angiogenic and growth factors, we measured VEGF, hepatocyte growth factor (HGF), insulin-like growth factor-1 (IGF-1), and adrenomedullin (AM) levels in conditioned medium 24 hours after medium replacement. VEGF, HGF, and IGF-1 were measured by enzyme immunoassay (VEGF immunoassay, R&D Systems Inc; rat HGF enzyme immunoassay, Institute of Immunology Co, Ltd; and active rat IGF-1 enzyme immunoassay, Diagnostic Systems Laboratories, Inc). AM level was measured with a radioimmu-

noassay kit (Shionogi Co), as reported previously.¹⁹ The amounts of these products produced by MSCs were compared with those produced by bone marrow-derived mononuclear cells (MNCs) because MNCs have commonly been used for regenerative therapy.¹⁹⁻²¹ There was no significant difference in cell viability between MSCs and MNCs 24 hours after seeding ($88\pm 5\%$ versus $85\pm 4\%$ by trypan blue solution). In vivo, circulating levels of VEGF, HGF, IGF-1, and AM were measured before and 24 hours after administration of MSCs or vehicle ($n=6$ from each group).

Statistical Analysis

Numerical values are expressed as mean \pm SEM unless otherwise indicated. Comparisons of parameters between 2 groups were made with unpaired Student *t* test. Comparisons of parameters among 3 groups were made with a 1-way ANOVA, followed by the Scheffe multiple-comparison test. Comparisons of changes in parameters among the 3 groups were made by a 2-way ANOVA for repeated measures, followed by the Scheffe multiple-comparison test. A value of $P<0.05$ was considered significant.

Results

Characterization of Cultured MSCs

Most cultured MSCs expressed CD29 and CD90 (Figure 1). In contrast, the majority of MSCs were negative for CD31, CD34, CD45, and SMA. Some of the MSCs expressed c-Kit and vimentin.

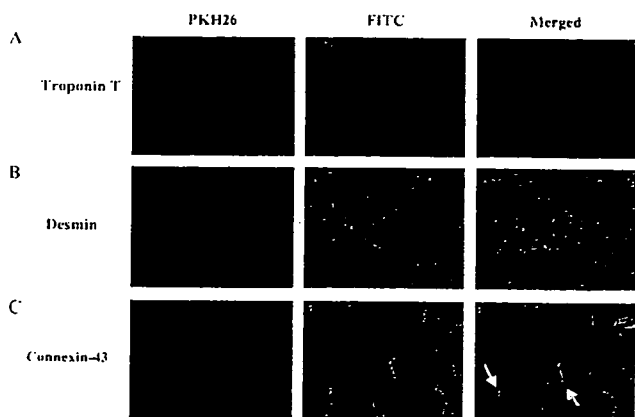


Figure 2. Differentiation of transplanted MSCs into cardiomyocytes. Transplanted MSCs were engrafted in the myocardium and stained for cardiac troponin T (A) and desmin (B). Engrafted MSCs also expressed connexin-43, a gap junction protein, at contact points with native cardiac myocytes (left arrow) and other transplanted cells (right arrow) (C). Magnification $\times 400$.

Myogenesis and Angiogenesis Induced by MSCs

Red fluorescence-labeled MSCs were transplanted into the myocardium 5 weeks after immunization. Four weeks after transplantation, MSCs were engrafted into the myocardium (Figure 2). Immunofluorescence demonstrated that transplanted MSCs were positive for the cardiac markers cardiac troponin T and desmin (Figure 2). Transplanted MSCs also expressed connexin-43, a gap junction protein, at contact points with native cardiac myocytes as well as with MSCs. FACS analysis of isolated heart cells demonstrated that $8 \pm 1\%$ of transplanted MSCs were double-positive for PKH26 and troponin T. These results suggest that a small number of transplanted MSCs can differentiate into cardiomyocytes.

Some transplanted MSCs formed vascular structures in the myocardium and were positive for von Willebrand factor (Figure 3A). Other MSCs were positive for SMA and participated in vessel formation as mural cells (Figure 3B). Alkaline phosphatase staining of the ischemic myocardium showed marked augmentation of neovascularization in the MSC-treated DCM group (Figures 4A–4C). Quantitative analysis demonstrated that capillary density was significantly



Figure 3. Differentiation of transplanted MSCs into vascular endothelial cells and smooth muscle cells. Some of the transplanted MSCs were positive for von Willebrand factor (vWF, A) and SMA (B) and formed vascular structures (A and B). Scale bars = 10 μm .

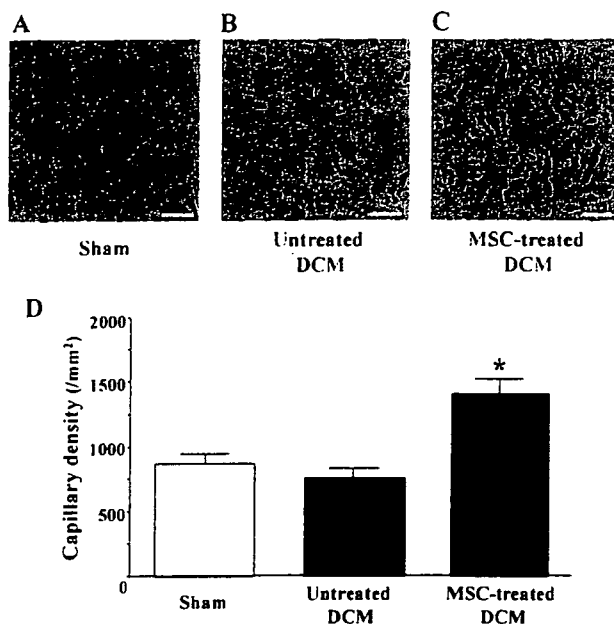


Figure 4. A–C, Representative samples of alkaline phosphatase staining of myocardium. Magnification, $\times 200$. Scale bars = 10 μm . D, Quantitative analysis of capillary density in the myocardium. Data are mean \pm SEM * $P < 0.05$ vs untreated DCM group.

higher in the MSC-treated DCM group than in the untreated DCM group (Figure 4D).

Angiogenic, Antiapoptotic, and Mitogenic Factors Released From MSCs

After 24 hours of culture, MSCs secreted large amounts of angiogenic and antiapoptotic factors, including VEGF, HGF, and AM (Figure 5). Compared with MNCs that have commonly been used for regenerative therapy,^{20–22} MSCs secreted 4-fold more VEGF and 5-fold more HGF. Similarly, MSCs secreted 6-fold more AM, an angiogenic and antiapoptotic peptide, compared with MNCs. MSCs also secreted a large amount, 10-fold greater than MNCs, of IGF-1, a growth hormone mediator for myocardial growth (Figure 5). Transplantation of MSCs significantly increased circulating VEGF (45.8 ± 1.6 to 68.5 ± 3.6 pg/mL, $P < 0.05$), HGF (431.8 ± 56.6 to 517.2 ± 67.1 pg/mL, $P < 0.05$), and AM (23.4 ± 0.8 to 41.2 ± 4.8 pg/mL, $P < 0.05$) 24 hours after transplantation, although vehicle injection did not alter these parameters. Serum IGF-1 tended to increase after MSC transplantation (938.1 ± 151.6 to 1063.5 ± 116.9 pg/mL, $P = \text{NS}$), but this increase did not reach statistical significance.

Hemodynamic Effects of MSC Transplantation

Nine weeks after immunization, LV end-diastolic pressure showed a marked elevation in the untreated DCM group; this elevation was significantly attenuated in the MSC-treated DCM group (Figure 6A). LV maximum dP/dt was significantly lower in the untreated DCM group than in the sham group (Figure 6B). However, LV maximum dP/dt was significantly improved 4 weeks after MSC transplantation. There was no significant difference in heart rate or mean arterial pressure among the 3 groups (the Table). Echocardiographic studies demonstrated LV dysfunction and dilation

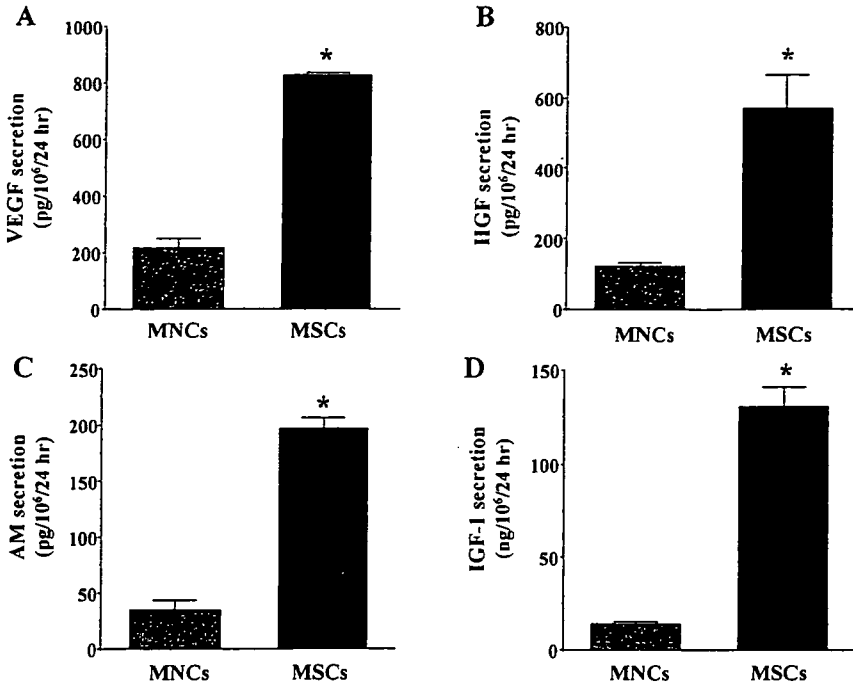


Figure 5. A–D, Angiogenic, antiapoptotic, and mitogenic factors produced by MSCs and bone marrow–derived MNCs). Compared with MNCs, MSCs secreted large amounts of VEGF, HGF, AM, and IGF-1. **P*<0.05 vs MNCs.

in the untreated DCM group, as indicated by a decrease in percent fractional shortening and an increase in LV diastolic dimension (Figure 6C and 6D). However, MSC transplantation increased percent fractional shortening and inhibited the increase in LV diastolic dimension.

Reduction of Myocardial Fibrosis by MSC Transplantation

Masson’s trichrome staining demonstrated modest myocardial fibrosis in the untreated DCM group (Figure 7A). However,

MSC transplantation significantly attenuated the development of myocardial fibrosis. Quantitative analysis also demonstrated that the collagen volume fraction in the MSC-treated DCM group was significantly smaller than that in the untreated DCM group (Figure 7B). Western blot analysis showed that myocardial contents of MMP-2 and MMP-9 in the untreated DCM were significantly increased compared with those in the sham group (Figure 7C–E). However, the increases in MMP-2 and MMP-9 levels were attenuated by MSC transplantation, although the change in MMP-9 did not reach statistical significance.

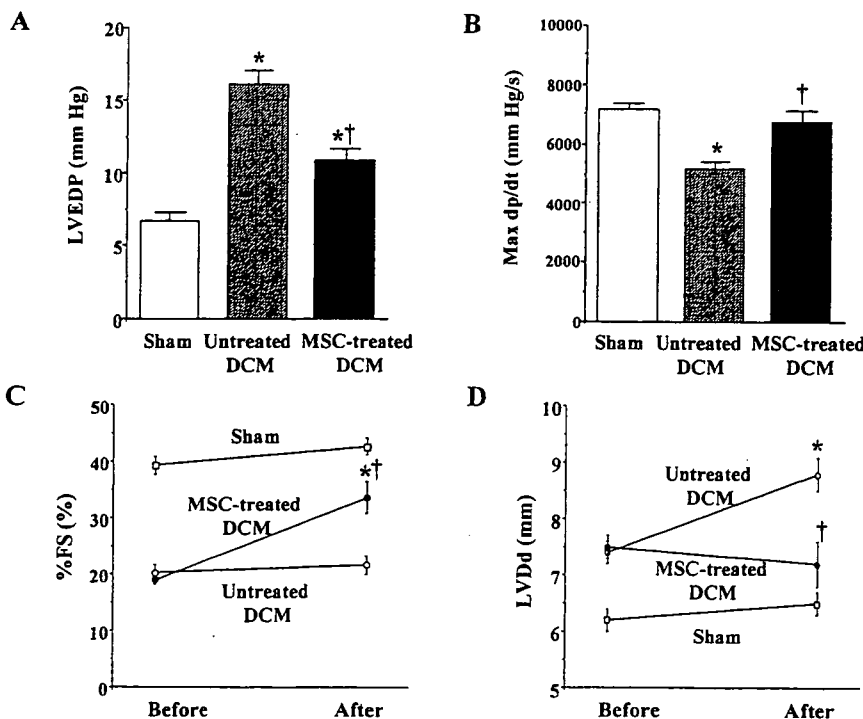


Figure 6. A and B, Effects of MSC transplantation on hemodynamic parameters. LVEDP indicates LV end-diastolic pressure; Max *dp/dt*, LV maximum *dp/dt*. Data are mean±SEM. **P*<0.05 vs sham group; †*P*<0.05 vs untreated DCM group. C and D, Changes in echocardiographic parameters induced by MSC transplantation. %FS indicates LV fractional shortening. Data are mean±SEM **P*<0.05 vs before transplantation; †*P*<0.05 vs the time-matched untreated DCM group.

Physiological Profiles of the 3 Experimental Groups

	Sham	Untreated DCM	MSC-Treated DCM
n	10	10	10
Body wt, g	421 ± 8	372 ± 4*	389 ± 5*
LV wt/body wt, g/kg	1.91 ± 0.05	2.18 ± 0.06*	2.05 ± 0.05
RV wt/body wt, g/kg	0.55 ± 0.01	0.68 ± 0.02*	0.60 ± 0.03†
Heart rate, bpm	403 ± 10	432 ± 15	417 ± 12
Mean arterial pressure, mm Hg	134 ± 2	123 ± 3	132 ± 5

wt indicates weight; RV, right ventricle. Sham-operated rats were given vehicle only. The untreated DCM group included DCM rats treated with vehicle. The MSC-treated DCM group included DCM rats treated with MSCs. Data are mean ± SEM.

*P < 0.05 vs sham group; †P < 0.05 vs untreated DCM group.

Discussion

In the present study, we have demonstrated the following effects of MSC transplantation in a rat model of DCM: (1) induction of myogenesis and angiogenesis; (2) differentiation of transplanted MSCs into cardiomyocytes, vascular endothelial cells, and smooth muscle cells; (3) secretion of large amounts of VEGF, HGF, AM, and IGF-1; (4) improvement of cardiac function and inhibition of ventricular remodeling; and (5) decrease in collagen volume fraction in the myocardium.

Earlier studies have shown that transplantation of MSCs improves cardiac function in experimental models of ischemic heart disease.^{9,23} However, little information is available about the therapeutic potential of MSCs for chronic heart failure due to DCM. Previous studies have shown that porcine cardiac myosin-induced myocarditis progresses to a chronic phase resembling DCM.^{13,14} Thus, we used this model 5 weeks after immunization as an example of experimental DCM.

In the present study, transplanted MSCs were engrafted into the myocardium in a rat model of DCM. Four weeks after transplantation, some of the engrafted MSCs were positively

stained for cardiac troponin T and desmin. Transplanted MSCs also expressed connexin-43, a gap junction protein, at contact points with native cardiac myocytes as well as with MSCs. These results suggest that MSCs differentiate into cardiomyocytes in the myocardium and form connections with native cardiomyocytes in rats with DCM. Unlike earlier studies that have used a model of myocardial infarction,^{7,9,23} we used a rat model of DCM to demonstrate the engraftment and cardiogenic differentiation of MSCs. Importantly, MSC transplantation improved cardiac function in these rats, as indicated by a significant decrease in LV end-diastolic pressure and an increase in LV dP/dt_{max} . Thus, the improvement in cardiac function may be a result of MSC-induced myocardial regeneration; however, further studies are necessary to investigate the mechanisms by which MSCs develop into cardiac myocyte-like cells.

Some of the transplanted MSCs were positive for a vascular endothelial cell marker and participated in vessel formation. MSC transplantation significantly increased capillary density in the myocardium. SMA staining revealed that MSCs differentiated into vascular smooth muscle cells, which play an important role in vessel maturation. Earlier studies have shown that transplantation of MNCs induces therapeutic angiogenesis in patients with limb ischemia or ischemic heart disease.²⁰⁻²² The angiogenic potential of MNCs is mediated at least in part by production by the cells of a variety of angiogenic factors.²⁴ Although MSCs have also been shown to produce VEGF,^{10,25} there has been no study to compare their production between MSCs and MNCs. The present study demonstrated that MSCs secreted ≈4-fold more VEGF compared with MNCs. Furthermore, MSCs secreted large amounts of HGF and AM, potent angiogenic factors.²⁶⁻³⁰ Taking these findings together, MSCs may contribute to neovascularization in the myocardium not only through their ability to generate capillary-like structures but also through growth factor-mediated paracrine regulation. Myocardial blood flow abnormalities have been documented in patients with heart failure caused by DCM.¹² Thus, it is possible that MSC-induced neovascularization contributes to improvement in cardiac function.

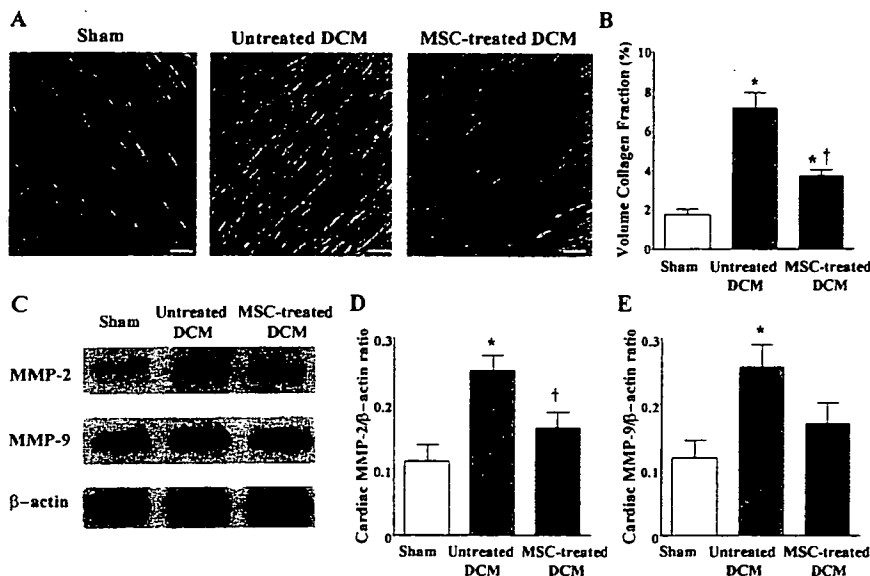


Figure 7. Effects of MSC transplantation on myocardial fibrosis. A, Photomicrographs show representative myocardial sections stained with Masson's trichrome. Scale bars = 10 μm. B, Quantitative analysis demonstrated that the collagen volume fraction in the MSC-treated DCM group was significantly smaller than that in the untreated DCM group. C, Representative Western blots for MMPs-2 and -9 and β-actin in the heart. D and E, Quantitative analysis of cardiac tissue contents of MMP-2 and -9. Data are mean ± SEM *P < 0.05 vs sham group; †P < 0.05 vs untreated DCM group.

HGF has not only angiogenic but also cardioprotective effects, including antiapoptotic, mitogenic, and antifibrotic activities.^{26,27} HGF gene transfer into the myocardium improves myocardial function and geometry.²⁸ In particular, the antifibrotic effects of HGF through inhibition of transforming growth factor- β expression is beneficial for heart failure. Cultured MSCs secreted a large amount of HGF. In vivo, transplantation of MSCs slightly increased plasma HGF in rats. It significantly attenuated the development of myocardial fibrosis in a rat model of DCM. These results suggest that MSC-derived HGF may contribute to improvements in cardiac function partly through its antifibrotic effects.

MSCs also produced AM, a potent vasodilator and cardioprotective peptide.²⁹ We have shown that AM prevents cardiomyocyte apoptosis through the phosphatidylinositol 3-kinase/Akt-dependent pathway¹⁶ and that it has potent angiogenic effects.³⁰ AM inhibits proliferation of cardiac fibroblasts through the cAMP-dependent pathway.³¹ Administration of AM inhibits LV remodeling and improves cardiac function in heart failure.³²⁻³⁴ In the present study, cultured MSCs secreted a large amount of AM in vitro. In vivo, transplantation of MSCs markedly increased plasma AM level. Taken together, these findings suggest that MSCs may exert their cardioprotective effects through AM-mediated paracrine regulation.

IGF-1, a growth hormone mediator, plays an important role in myocardial and skeletal muscle growth.^{35,36} Administration of IGF-1 improves cardiac function after myocardial infarction through enhancement of myocardial growth.³⁷ Its protective and antiapoptotic properties have been demonstrated in different models of myocardial ischemia.³⁸ Furthermore, IGF-1 exerts Ca²⁺-dependent, positive inotropic effects through a phosphatidylinositol 3-kinase-dependent pathway.³⁹ Interestingly, the present study demonstrated that MSCs secreted significant amounts of IGF-1 in vitro, 10-fold greater than MNCs. These findings raise the possibility that MSC-derived IGF-1 may participate in myocardial growth and enhancement of myocardial contractility in a rat model of DCM.

MMPs also play a crucial role in extracellular remodeling in heart failure.⁴⁰ In fact, pharmacological inhibition of MMP activities prevents progressive LV remodeling in an animal model of heart failure.⁴¹ In the present study, cardiac MMP-2 and MMP-9 were increased in rats with DCM, which is consistent with recent findings in patients with heart failure.^{40,42} Interestingly, MSC transplantation attenuated the increases in cardiac MMP-2 and MMP-9 in a rat model of DCM. Although the underlying mechanisms remain unclear, MSC transplantation may influence extracellular remodeling in heart failure.

The present study has some limitations. First, immunohistochemical evidence suggests differentiation of MSCs into cardiomyocytes, vascular endothelial cells, and smooth muscle cells. However, further studies are necessary to convincingly demonstrate differentiation of MSCs into a specific cell type. Second, the model of DCM used in this study was an injury model, and the effects of treatment may be related to attenuation of the injury rather than to the established cardiomyopathy. Nonetheless, the experiment was performed 5 to 9 weeks after myosin injection, by which time inflammatory changes were hardly observed and had been replaced by fibrosis.⁴³

Conclusions

MSC transplantation improved cardiac function in a rat model of DCM, possibly through induction of myogenesis and angiogenesis, as well as by inhibition of myocardial fibrosis. The beneficial effects of MSCs may be mediated at least in part by their differentiation into cardiomyocytes and vascular cells and by their ability to supply large amounts of angiogenic, antiapoptotic, and mitogenic factors. Thus, MSC transplantation has potential as a new therapeutic strategy for the treatment of DCM.

Acknowledgments

This work was supported by research grants for cardiovascular disease (16C-6) and Human Genome Tissue Engineering 009 from the Ministry of Health, Labor and Welfare; the Industrial Technology Research Grant Program in '03 from the New Energy and Industrial Technology Development Organization of Japan; a research grant from the Japan Cardiovascular Research Foundation; and Promotion of Fundamental Studies in Health Science of the Organization for Pharmaceutical Safety and Research of Japan.

References

- Cohn JN. The management of chronic heart failure. *N Engl J Med*. 1996;335:490-498.
- Dec GW, Fuster V. Idiopathic dilated cardiomyopathy. *N Engl J Med*. 1994;331:1564-1575.
- Beltrami AP, Urbanek K, Kajstura J, Yan SM, Finato N, Bussani R, Nadal-Ginard B, Silvestri F, Leri A, Beltrami CA, Anversa P. Evidence that human cardiac myocytes divide after myocardial infarction. *N Engl J Med*. 2001;344:1750-1757.
- Pittenger MF, Mackay AM, Beck SC, Jaiswal RK, Douglas R, Mosca JD, Moorman MA, Simonetti DW, Craig S, Marshak DR. Multilineage potential of adult human mesenchymal stem cells. *Science*. 1999;284:143-147.
- Reyes M, Dudek A, Jahagirdar B, Koodie L, Marker PH, Verfaillie CM. Origin of endothelial progenitors in human postnatal bone marrow. *J Clin Invest*. 2002;109:337-346.
- Toma C, Pittenger MF, Cahill KS, Byrne BJ, Kessler PD. Human mesenchymal stem cells differentiate to a cardiomyocyte phenotype in the adult murine heart. *Circulation*. 2002;105:93-98.
- Mangi AA, Noiseux N, Kong D, He H, Rezvani M, Ingwall JS, Dzau VJ. Mesenchymal stem cells modified with Akt prevent remodeling and restore performance of infarcted hearts. *Nat Med*. 2003;9:1195-1201.
- Makino S, Fukuda K, Miyoshi S, Konishi F, Kodama H, Pan J, Sano M, Takahashi T, Hori S, Abe H, Hata J, Umezawa A, Ogawa S. Cardiomyocytes can be generated from marrow stromal cells in vitro. *J Clin Invest*. 1999;103:697-705.
- Shake JG, Gruber PJ, Baumgartner WA, Senechal G, Meyers J, Redmond JM, Pittenger MF, Martin BJ. Mesenchymal stem cell implantation in a swine myocardial infarct model: engraftment and functional effects. *Ann Thorac Surg*. 2002;73:1919-1925.
- Al-Khalidi A, Al-Sabti H, Galipeau J, Lachapelle K. Therapeutic angiogenesis using autologous bone marrow stromal cells: improved blood flow in a chronic limb ischemia model. *Ann Thorac Surg*. 2003;75:204-209.
- Al-Khalidi A, Eliopoulos N, Martineau D, Lejeune L, Lachapelle K, Galipeau J. Postnatal bone marrow stromal cells elicit a potent VEGF-dependent neoangiogenic response in vivo. *Gene Ther*. 2003;10:621-629.
- Parodi O, De Maria R, Oltrona L, Testa R, Sambucetti G, Roghi A, Merli M, Belingheri L, Accinni R, Spinelli F, Pellegrini A, Baroldi G. Myocardial blood flow distribution in patients with ischemic heart disease or dilated cardiomyopathy undergoing heart transplantation. *Circulation*. 1993;88:509-522.
- Kodama M, Zhang S, Hanawa H, Saeki M, Inomata T, Suzuki K, Koyama S, Shibata A. Effects of 15-deoxyspergualin on experimental autoimmune giant cell myocarditis of the rat. *Circulation*. 1995;91:1116-1122.
- Watanabe K, Ohta Y, Nakazawa M, Higuchi H, Hasegawa G, Naito M, Fuse K, Ito M, Hirono S, Tanabe N, Hanawa H, Kato K, Kodama M, Aizawa Y. Low dose carvedilol inhibits progression of heart failure in rats with dilated cardiomyopathy. *Br J Pharmacol*. 2000;130:1489-1495.

15. Nagaya N, Uematsu M, Kojima M, Ikeda Y, Yoshihara F, Shimizu W, Hosoda H, Hirota Y, Ishida H, Mori H, Kangawa K. Chronic administration of ghrelin improves left ventricular dysfunction and attenuates development of cardiac cachexia in rats with heart failure. *Circulation*. 2001;104:1430–1435.
16. Okumura H, Nagaya N, Itoh T, Okano I, Hino J, Mori K, Tsukamoto Y, Ishibashi-Ueda H, Miwa S, Tambara K, Toyokuni S, Yutani C, Kangawa K. Adrenomedullin infusion attenuates myocardial ischemia/reperfusion injury through the phosphatidylinositol 3-kinase/Akt-dependent pathway. *Circulation*. 2004;109:242–248.
17. Messina LM, Podrazik RM, Whitehill TA, Ekhterae D, Brothers TE, Wilson JM, Burkel WE, Stanley JC. Adhesion and incorporation of lacZ-transduced endothelial cells into the intact capillary wall in the rat. *Proc Natl Acad Sci U S A*. 1992;89:12018–12022.
18. Harada M, Itoh H, Nakagawa O, Ogawa Y, Miyamoto Y, Kuwahara K, Ogawa E, Igaki T, Yamashita J, Masuda I, Yoshimasa T, Tanaka I, Saito Y, Nakao K. Significance of ventricular myocytes and nonmyocytes interaction during cardiocyte hypertrophy: evidence for endothelin-1 as a paracrine hypertrophic factor from cardiac nonmyocytes. *Circulation*. 1997;96:3737–3744.
19. Ohta H, Tsuji T, Asai S, Sasakura K, Teraoka H, Kitamura K, Kangawa K. A simple immunoradiometric assay for measuring the entire molecules of adrenomedullin in human plasma. *Clin Chim Acta*. 1999;287:B131–B143.
20. Murohara T, Ikeda H, Duan J, Shintani S, Sasaki K, Eguchi H, Onitsuka I, Matsui K, Imaizumi T. Transplanted cord blood-derived endothelial precursor cells augment postnatal neovascularization. *J Clin Invest*. 2000;105:1527–1536.
21. Tateishi-Yuyama E, Matsubara H, Murohara T, Ikeda U, Shintani S, Masaki H, Amano K, Kishimoto Y, Yoshimoto K, Akashi H, Shimada K, Iwasaka T, Imaizumi T. Therapeutic Angiogenesis using Cell Transplantation (TACT) Study Investigators. Therapeutic angiogenesis for patients with limb ischaemia by autologous transplantation of bone-marrow cells: a pilot study and a randomised controlled trial. *Lancet*. 2002;360:427–435.
22. Tse HF, Kwong YL, Chan JK, Lo G, Ho CL, Lau CP. Angiogenesis in ischaemic myocardium by intramyocardial autologous bone marrow mononuclear cell implantation. *Lancet*. 2003;361:47–49.
23. Min JY, Sullivan MF, Yang Y, Zhang JP, Converso KL, Morgan JP, Xiao YF. Significant improvement of heart function by cotransplantation of human mesenchymal stem cells and fetal cardiomyocytes in postinfarcted pigs. *Ann Thorac Surg*. 2002;74:1568–1575.
24. Kamihata H, Matsubara H, Nishiue T, Fujiyama S, Tsutsumi Y, Ozono R, Masaki H, Mori Y, Iba O, Tateishi E, Kosaki A, Shintani S, Murohara T, Imaizumi T, Iwasaka T. Implantation of bone marrow mononuclear cells into ischemic myocardium enhances collateral perfusion and regional function via side supply of angioblasts, angiogenic ligands, and cytokines. *Circulation*. 2001;104:1046–1052.
25. Kinnaird T, Stabile E, Burnett MS, Lee CW, Barr S, Fuchs S, Epstein SE. Marrow-derived stromal cells express genes encoding a broad spectrum of arteriogenic cytokines and promote in vitro and in vivo arteriogenesis through paracrine mechanisms. *Circ Res*. 2004;94:678–685.
26. Nakamura T, Nishizawa T, Hagiya M, Seki T, Shimonishi M, Sugimura A, Tashiro K, Shimizu S. Molecular cloning and expression of human hepatocyte growth factor. *Nature*. 1989;342:440–443.
27. Nakamura T, Mizuno S, Matsumoto K, Sawa Y, Matsuda H, Nakamura T. Myocardial protection from ischemia/reperfusion injury by endogenous and exogenous HGF. *J Clin Invest*. 2000;106:1511–1519.
28. Li Y, Takemura G, Kosai K, Yuge K, Nagano S, Esaki M, Goto K, Takahashi T, Hayakawa K, Koda M, Kawase Y, Maruyama R, Okada H, Minatoguchi S, Mizuguchi H, Fujiwara T, Fujiwara H. Postinfarction treatment with an adenoviral vector expressing hepatocyte growth factor relieves chronic left ventricular remodeling and dysfunction in mice. *Circulation*. 2003;107:2499–2506.
29. Kitamura K, Kangawa K, Kawamoto M, Ichiki Y, Nakamura S, Matsuo H, Eto T. Adrenomedullin: a novel hypotensive peptide isolated from human pheochromocytoma. *Biochem Biophys Res Commun*. 1993;192:553–560.
30. Tokunaga N, Nagaya N, Shirai M, Tanaka E, Ishibashi-Ueda H, Harada-Shiba M, Kanda M, Ito T, Shimizu W, Tabata Y, Uematsu M, Nishigami K, Sano S, Kangawa K, Mori H. Adrenomedullin gene transfer induces therapeutic angiogenesis in a rabbit model of chronic hind limb ischemia: benefits of a novel nonviral vector, gelatin. *Circulation*. 2004;109:526–531.
31. Tsuruda T, Kato J, Kitamura K, Kawamoto M, Kuwasako K, Imamura T, Koiwaya Y, Tsuji T, Kangawa K, Eto T. An autocrine or a paracrine role of adrenomedullin in modulating cardiac fibroblast growth. *Cardiovasc Res*. 1999;43:958–967.
32. Nishikimi T, Yoshihara F, Horinaka S, Kobayashi N, Mori Y, Tadokoro K, Akimoto K, Minamino N, Kangawa K, Matsuoka H. Chronic administration of adrenomedullin attenuates tension from left ventricular hypertrophy to heart failure in rats. *Hypertension*. 2003;42:1034–1041.
33. Nakamura R, Kato J, Kitamura K, Onitsuka H, Imamura T, Cao Y, Marutsuka K, Asada Y, Kangawa K, Eto T. Adrenomedullin administration immediately after myocardial infarction ameliorates progression of heart failure in rats. *Circulation*. 2004;110:426–431.
34. Nagaya N, Satoh T, Nishikimi T, Uematsu M, Furuichi S, Sakamaki F, Oya H, Kyotani S, Nakanishi N, Goto Y, Masuda Y, Miyatake K, Kangawa K. Hemodynamic, renal, and hormonal effects of adrenomedullin infusion in patients with congestive heart failure. *Circulation*. 2000;101:498–503.
35. Fuller J, Mynett JR, Sugden PH. Stimulation of cardiac protein synthesis by insulin-like growth factors. *Biochem J*. 1992;282:85–90.
36. Florini JR, Ewton DZ, Coolican SA. Growth hormone and the insulin-like growth factor system in myogenesis. *Endocr Rev*. 1996;17:481–517.
37. Cittadini A, Stromer H, Katz SE, Clark R, Moses AC, Morgan JP, Douglas PS. Differential cardiac effects of growth hormone and insulin-like growth factor-1 in the rat: a combined in vivo and in vitro evaluation. *Circulation*. 1996;93:800–809.
38. Li Q, Li B, Wang X, Leri A, Jana KP, Liu Y, Kajstura J, Baserga R, Anversa P. Overexpression of insulin-like growth factor-1 in mice protects from myocyte death after infarction, attenuating ventricular dilation, wall stress, and cardiac hypertrophy. *J Clin Invest*. 1997;100:1991–1999.
39. von Lewinski D, Voss K, Hulsmann S, Kogler H, Pieske B. Insulin-like growth factor-1 exerts Ca²⁺-dependent positive inotropic effects in failing human myocardium. *Circ Res*. 2003;92:169–176.
40. Thomas CV, Coker ML, Zellner JL, Handy JR, Crumbley AJ 3rd, Spinale FG. Increased matrix metalloproteinase activity and selective upregulation in LV myocardium from patients with end-stage dilated cardiomyopathy. *Circulation*. 1998;97:1708–1715.
41. Spinale FG, Coker ML, Krombach SR, Mukherjee R, Hallak H, Houck WV, Clair MJ, Kribbs SB, Johnson LL, Peterson JT, Zile MR. Matrix metalloproteinase inhibition during the development of congestive heart failure: effects on left ventricular dimensions and function. *Circ Res*. 1999;85:364–376.
42. Spinale FG, Coker ML, Heung LJ, Bond BR, Gunasinghe HR, Etoh T, Goldberg AT, Zellner JL, Crumbley AJ. A matrix metalloproteinase induction/activation system exists in the human left ventricular myocardium and is upregulated in heart failure. *Circulation*. 2000;102:1944–1949.
43. Kodama M, Matsumoto Y, Fujiwara M, Zhang SS, Hanawa H, Itoh E, Tsuda T, Izumi T, Shibata A. Characteristics of giant cells and factors related to the formation of giant cells in myocarditis. *Circ Res*. 1991;69:1042–1050.

CLINICAL PERSPECTIVE

Transplantation of stem or progenitor cells has the potential to improve and restore cardiac function. To date, experimenters investigating the possible therapeutic effects of stem cells in the heart have used models of infarction, and little information is available about the therapeutic potential of cell transplantation for heart failure due to dilated cardiomyopathy. In the present study, we demonstrated that transplantation of stem cells improved cardiac function in a model of myocarditis. We found evidence that stem cells may work to improve heart function by both myogenesis and angiogenesis while inhibiting myocardial fibrosis. Based on our data, part of the mechanism for this improvement may occur through the action of stem cells as a source of growth factors and cytokines in the heart. This study supports the overall notion that mesenchymal stem cells transplanted into the failing heart have potential as a new therapeutic strategy for the treatment of dilated cardiomyopathy.

EXOGENOUS NITRIC OXIDE CENTRALLY ENHANCES PULMONARY REACTIVITY IN THE NORMAL AND HYPERTENSIVE RAT

Daryl O Schwenke,* James T Pearson,* Hirotugu Tsuchimochi,* Hidezo Mori* and Mikiyasu Shirai†

*Department of Cardiac Physiology, National Cardiovascular Center Research Institute, Suita, Osaka and

†Faculty of Health Sciences, Hiroshima International University, Hiroshima, Japan

SUMMARY

1. Chronic hypoxia causes sustained pulmonary hypertension and, although impairment of the pulmonary endothelial nitric oxide (NO) pathway has been implicated, no study has described the central role of NO in modulating pulmonary vascular tone and reactivity. Centrally, NO inhibits sympathetic outflow, so we hypothesised that central NO would modulate pulmonary vascular tone and its reactivity to acute hypoxia, especially in the hypertensive state.

2. Male adult Sprague-Dawley rats were exposed to normoxia (N) or chronic hypoxia (CH; 12% O₂) for 14 days. Mean pulmonary arterial pressure (MPAP), systemic mean arterial blood pressure (MABP), cardiac output and heart rate were then measured in pentobarbitone-anaesthetized, artificially ventilated rats. The N and CH rats were exposed to acute hypoxia (10% O₂ for 4 min) after the intracerebroventricular (i.c.v.) administration of artificial cerebrospinal fluid (control) and then again after either i.c.v. N^G-nitro-L-arginine methyl ester (L-NAME; 150 µg in 10 µL) or 3-morpholino-sydnonimine hydrochloride (SIN-1; 100 µg in 10 µL).

3. Chronic hypoxia caused pulmonary hypertension (MPAP 20 ± 1 vs 30 ± 1 mmHg in N and CH rats, respectively) and attenuated acute hypoxic pulmonary vasoconstriction (HPV). Central inhibition of NO synthesis (by L-NAME) did not alter baseline MPAP or the acute HPV in either N or CH rats, but it did elevate MABP. The NO donor SIN-1 did not alter baseline MPAP, but it did enhance (N rats) or restore (CH rats) the HPV and decreased MABP.

4. The results of the present study indicate that central NO has a limited role in the tonic modulation of MPAP during normoxia and after chronic hypoxia. However, the acute HPV seems to be enhanced by exogenous NO.

Key words: chronic hypoxia, nitric oxide, pulmonary vasoconstriction, sympathetic nervous system.

INTRODUCTION

Acute alveolar hypoxia causes pulmonary vasoconstriction that is reversible upon re-oxygenation. However, during chronic hypoxia, as is the case with several chronic pulmonary pathological conditions, elevated shear stress within the pulmonary vasculature causes endothelial cell injury/dysfunction,¹ smooth muscle cell proliferation² and, inevitably, the irreversible remodelling of the pulmonary vasculature.^{3,4} The consequential sustained increase in pulmonary arterial pressure (PAP) increases the workload of the heart and is therefore closely associated with heart failure and increased mortality.

Although the exact cellular mechanisms responsible for the pathogenesis of chronic hypoxia-induced pulmonary arterial hypertension are unknown, alterations in the endothelial nitric oxide (NO) pathway have been implicated as a significant contributing factor.^{5,6} Nitric oxide is a potent vasodilator and an inhibitor of vascular remodelling.^{7–9} Nitric oxide is produced from L-arginine in a reaction catalysed by isoenzymes of NO synthase (NOS). The synthesis of NO is blocked by several L-arginine analogues, including N^G-nitro-L-arginine methyl ester (L-NAME), which competitively and stereoselectively inhibit the generation of NO from L-arginine.¹⁰

A reduction in the production of NO has been implicated in the pathophysiology of pulmonary hypertension.^{6,8} Endothelial NOS (eNOS)-knockout mice have an increased risk of pulmonary hypertension,^{11–13} whereas the hypoxia-induced pulmonary hypertension is attenuated in transgenic mice that overexpress eNOS.¹⁴ In addition, chronic hypoxia limits endogenous NO synthesis,¹⁵ despite an increase in NOS expression.^{16–18}

Nitric oxide is produced not only peripherally, but also centrally within various parts of the brain, including the nucleus tractus solitarius (NTS) of the medulla oblongata and the ventrolateral medulla, the cardiovascular regulatory centres.^{19–21} Therefore, NO is considered to be involved in the neural regulation of blood pressure, independent of its direct effects on the endothelium of blood vessels.²² A review by Patel *et al.*²³ reported that the general consensus in the literature was that NO acts as a sympatho-inhibitory substance within the central nervous system. Therefore, central NO inhibition increases sympathetic outflow and, subsequently, arterial blood pressure.^{24,25}

The central role of NO in modulating pulmonary vasculature, especially in pathological conditions (e.g. pulmonary hypertension), is still incompletely understood. Yet, as evidence accumulates in support of central NO as an important regulator

Correspondence: Daryl O Schwenke, Department of Cardiac Physiology, National Cardiovascular Center Research Institute, 5-7-1 Fujishirodai, Suita, Osaka 565-8565, Japan. Email: schwenke@ri.ncvc.go.jp

Received 2 March 2005; revision 1 June 2005; accepted 17 July 2005.

© 2005 Blackwell Publishing Asia Pty Ltd

of cardiovascular function, the central role of NO in the modulation of the pulmonary vasculature needs to be addressed. Therefore, our first aim in the present study was to elucidate the role of NO in the central modulation of pulmonary vascular tone under normoxic conditions and after the development of chronic hypoxia-induced pulmonary hypertension. Nitric oxide is thought to have an important role in modulating the hypoxic pulmonary vasoconstriction (HPV) in response to acute hypoxic challenges.²⁶ However, there are conflicting reports as to whether the HPV response is accentuated or attenuated by pulmonary hypertension.^{6,27} Therefore, a second aim of the present study was to assess the acute HPV before and after chronic hypoxia and to determine whether central NO has a role in modulating this response.

METHODS

Animals

Experiments were conducted on 23 male Sprague-Dawley rats (8 weeks old; bodyweight approximately 200–280 g). Rats were divided into four groups, as follows: (i) group 1, normoxia (N) + L-NAME; (ii) group 2, chronic hypoxia (CH) + L-NAME; (iii) group 3, N + 3-morpholino-sydnimine hydrochloride (SIN-1); and (iv) group 4, CH + SIN-1. The CH rats were housed in a hypoxic chamber ($12.0 \pm 0.1\%$ O₂) continuously for 2 weeks, except for a 10 min interval each day when the chamber was cleaned. The N rats were housed in similar housing, except that N rats breathed room air. The hypoxic gas mixture was delivered to the hypoxic chamber (30 L capacity) at a flow rate of approximately 8 L/min. All rats were on a 12 h light/dark cycle at $25 \pm 1^\circ\text{C}$ and were provided with food and water *ad libitum*. All experiments were approved by the local Animal Ethics Committee and conducted in accordance with the guidelines of the Physiological Society of Japan (<http://www.soc.nii.ac.jp/psj/>).

Anaesthesia and surgery

Rats were initially anaesthetized with pentobarbitone sodium (45 mg/kg, i.p.) and supplementary doses of anaesthetic were administered periodically throughout the experimental protocol (15–30 mg/kg per h, i.p.) so as to maintain a constant surgical level of anaesthesia (assessed by using the limb withdrawal reflex test). Rectal temperature was maintained at 38°C using a rectal thermistor coupled to a thermostatically controlled heating pad.

Using a stereotaxic frame, the tip of a 27 gauge stainless steel cannula was positioned in the right lateral cerebral ventricle based on the coordinates of Paxinos and Watson²⁸ (0.8 mm posterior to the bregma, 1.5 mm lateral to the midline and 5.0 mm ventral to the skull surface). The distal end of the cannula was connected to a 0.5 mL syringe for subsequent drug administration. Correct positioning of the intracerebroventricular (i.c.v.) catheter was confirmed after each experiment by staining with Evans blue dye (10 μL).

The trachea was cannulated and the lungs ventilated with a rodent ventilator (SN-480-7; Shinano, Tokyo, Japan). The inspirate gas was enriched with O₂ (approximately 50% O₂) and the ventilator settings were adjusted (tidal volume (V_T) approximately 3.5 mL; frequency approximately 80 /min) to maintain arterial P_{CO2} normocapnic. The femoral artery and vein were cannulated for the measurement of systemic arterial blood pressure and drug administration, respectively. The arterial line contained heparinized saline (50 U/mL). A right thoracotomy was made between the second and third ribs and the conus of the right ventricle was exposed. A 23 gauge needle was used to pierce the ventricle wall and then the gel-filled sensing catheter of a telemetric transmitter (model TA11PA-C40; Data Sciences, St Paul, MN, USA) was inserted anteriorly into the right ventricle and advanced into the pulmonary artery. The catheter was fixed in position with a 7.0 Prolene suture to the pericardium. The aorta was bluntly dissected free from the pulmonary artery and a transonic perivascular flowprobe

(model 2RB; Transonic Systems, Ithaca, NY, USA) was positioned around the ascending aorta for the continuous measurement of cardiac output.

Drugs

Artificial cerebrospinal fluid (aCSF) was used as the vehicle for administering the NOS inhibitor L-NAME and the slow-releasing NO donor, 3-[4-morpholino]-sydnimine-hydrochloride (SIN-1). The aCSF (pH 7.36–7.43) was comprised of 150 mmol/L NaCl, 3.0 mmol/L KCl, 0.8 mmol/L MgCl₂, 1.4 mmol/L CaCl₂ and 1.0 mmol/L Na phosphate. Intracerebroventricular injections were given as a 10 μL bolus over 30 s. Intravenous (i.v.) injections were administered as a 0.2 mL bolus over 15 s, followed by a 0.1 mL saline flush.

Measurement of right ventricular weight

Immediately following the experiment, rats were killed by anaesthetic overdose, the heart was excised, the atria were removed and the right ventricle wall was separated from the left ventricle, including the septum. Tissues were blotted and weighed. Right and left ventricular weights were expressed as the ratio of the right ventricle to the left ventricular + septum weight ($W_{RV}/W_{LV+septum}$; Fulton's ratio).

Experimental protocols

Once all variables had stabilized after surgery (approximately 20 min), baseline values were recorded for 10 min in response to the i.c.v. administration of aCSF (10 μL). The inspirate was then switched to hypoxia (10% O₂ balanced by N₂) for 4 min. Upon recovery from acute hypoxia, rats received a bolus i.c.v. injection of either L-NAME (150 μg ; groups 1 and 2) or SIN-1 (100 μg ; groups 3 and 4). After 5 (L-NAME) or 10 min (SIN-1), the acute hypoxic test was repeated. After a further 10 min, once variables had recovered to prehypoxic values, rats (groups 1 and 2 only) received a bolus i.v. injection of L-NAME (50 mg/kg) and acute hypoxia was tested 10 min later.

Data acquisition and analysis

Pulmonary arterial pressure was measured using telemetry. The signal from the implanted transmitter (model TA11PA-C20; Data Sciences) was calibrated in reference to an input from an ambient-pressure monitor (C11PR; Data Sciences) and subsequently relayed to a personal computer. Cardiac output (CO) was measured continuously from the ascending aorta using a Transonic small animal blood flowmeter (model T206; Transonic Systems) with a flowprobe (model 2RB). Arterial blood pressure (ABP) was measured continuously with a Deltran pressure transducer (Utah Medical Products, Midvale, UT, USA) and the signal was relayed to a Powerlab bridge amplifier (ML117; ADInstruments, Tokyo, Japan).

The signals for ABP, CO and PAP were relayed from their respective units and sampled continuously at 200 Hz with an eight-channel MacLab/8s interface hardware system (ADInstruments) and recorded on a Macintosh Power Book G4 using Chart (v. 5.0.1; ADInstruments). Heart rate (HR) was derived from the arterial systolic peaks. Cardiac output was normalized (off-line) to 100 g bodyweight. Total systemic vascular resistance (SVR) and total pulmonary vascular resistance (PVR) were calculated by dividing mean ABP (MABP) and mean PAP (MPAP) by the normalized CO. A 10 block of data was analysed –60, –30 s and immediately before (time '0') acute hypoxic exposure and then after 20, 40, 60, 90, 120, 180 and 240 s of exposure to 10% O₂. Normoxic data for individual rats in each group were averaged from values acquired at –60, –30 s and at time 0. An arterial blood sample (0.1 mL) was extracted 5 min after the completion of surgery for analysis of arterial P_{CO2} using an ABL 605 blood gas analyser (Radiometer, Copenhagen, Denmark). An additional 0.1 mL was extracted to measure haematocrit.

Statistical analysis

All statistical analyses were conducted using Statview (v. 5.01; SAS Institute, Cary, NC, USA). All results are presented as the mean \pm SEM. Two-way ANOVA (repeated measures) was used to test significance for: (i) changes in each variable in response to 4 min of acute hypoxia; and (ii) whether the hypoxic response was altered by drug administration (i.c.v. or i.v.).

One-way ANOVA (factorial) was used to test for differences in baseline values for normoxic and chronic hypoxic groups of rats. Where statistical significance was reached, post hoc analyses were incorporated using the paired or unpaired *t*-test with Dunnett's correction for multiple comparisons. $P \leq 0.05$ was predetermined as the level of significance for all statistical analyses.

RESULTS

Chronic hypoxia induced pulmonary hypertension (Table 1), as evidenced by the observation that the MPAP and PVR of CH rats ($n = 11$) was 50 and 34% higher, respectively, than that of normoxic (N) rats ($n = 12$; $P < 0.01$). Consequently, CH rats developed right ventricular hypertrophy (Δ RV/LV + Sep ratio of 0.23). Chronic hypoxia did not significantly change MABP or CO, but it did cause a significant reduction in HR (Δ HR 37 b.p.m.; $P < 0.01$), suggesting that the development of right ventricular hypertrophy resulted in an increase in stroke volume. An increase in haematocrit (Δ Hct 18%; $P < 0.001$) also occurred in CH.

Responses to acute hypoxia

In N rats, acute exposure to 10% O₂ provoked an increase in MPAP, after a latency of 65–88 s, which reached a plateau after approxi-

mately 180 s (Fig. 1a). By 4 min, MPAP had increased significantly by $31 \pm 5\%$, in spite of a small, albeit not significant, decline in both HR ($6 \pm 1\%$) and CO ($16 \pm 6\%$), reflecting substantial pulmonary vasoconstriction ($67 \pm 13\%$ increase in PVR). Acute hypoxia also provoked a $56 \pm 2\%$ decrease in MABP by the end of the 4th min, which was primarily due to systemic vasodilatation ($46 \pm 3\%$ decrease in SVR; Fig. 1a). Although CH slightly altered baseline values (detailed above), the magnitude of the response to 4 min hypoxia for MABP, HR, CO and SVR was essentially the same for the CH and N groups of rats (Fig. 1a,b). However, the potent pulmonary vasoconstriction seen in N rats was abolished in CH rats. Consequently, exposure to 10% O₂ did not cause a significant increase in MPAP or PVR in CH rats.

Administration of L-NAME

The maximum cardiovascular responses following a single i.c.v injection of L-NAME are given in Table 2. In N rats, L-NAME caused a small (<3% increase) but consistent increase in PVR ($P < 0.05$), although MPAP was not significantly affected. In addition, L-NAME caused a maximal $15 \pm 4\%$ increase in MABP after 35 ± 8 s, which was solely attributed to systemic vasoconstriction ($16 \pm 4\%$ increase in SVR). All other variables were unaltered. The PVR, MABP and SVR responses were brief, returning to pre-L-NAME values within 4.5 min. Consequently, because acute hypoxia was tested 5 min after L-NAME injection, the prehypoxia baseline data were similar before and after L-NAME treatment. Furthermore, the magnitude of the cardiovascular responses to L-NAME for CH rats was statistically similar to that of N rats (Table 2). The i.c.v. administration of L-NAME did

Table 1 Baseline cardiovascular variables in rats exposed to normoxic or chronic hypoxia

	N rats	CH rats
MPAP (mmHg)	20.2 \pm 1.1	30.4 \pm 1.2**
MABP (mmHg)	106 \pm 6	118 \pm 4
CO (mL/min/100 g)	11.17 \pm 0.75	12.32 \pm 0.53
HR (b.p.m.)	416 \pm 8	379 \pm 11*
SVR (mmHg/mL per min per 100 g)	9.73 \pm 0.64	9.72 \pm 0.53
PVR (mmHg/mL per min per 100 g)	1.88 \pm 0.14	2.52 \pm 0.15*
RV/LV + Septum	0.31 \pm 0.01	0.55 \pm 0.02**
Haematocrit (%)	47 \pm 1	65 \pm 1**

Data are the mean \pm SEM. * $P < 0.01$, ** $P < 0.001$ compared with normoxia values.

N, normoxic rats (groups 1 and 3; $n = 12$); CH, chronic-hypoxic rats (12% O₂ for 2 weeks; groups 2 and 4; $n = 11$); MPAP, mean pulmonary arterial pressure; MABP, mean arterial blood pressure; CO, cardiac output; HR, heart rate; SVR, systemic vascular resistance; PVR, pulmonary vascular resistance; RV, right ventricle; LV, left ventricle.

Table 2 Maximum responses to intracerebroventricular N^G-nitro-L-arginine methyl ester (150 μ g in 10 μ L) in normoxic rats ($n = 7$) and chronic hypoxic rats ($n = 5$)

	Pre-L-NAME	Normoxia Max L-NAME	Pre-L-NAME	Chronic hypoxia Max L-NAME
MPAP (mmHg)	18.6 \pm 0.6	19.0 \pm 0.6	30.4 \pm 1.6	31.1 \pm 1.9
MABP (mmHg)	102 \pm 10	116 \pm 8**	110 \pm 5	120 \pm 5*
CO (mL/min per 100 g)	10.12 \pm 1.10	10.09 \pm 1.13	12.24 \pm 1.07	11.98 \pm 1.00
HR (b.p.m.)	413 \pm 10	416 \pm 9	373 \pm 13	376 \pm 14
SVR (mmHg/mL per min per 100 g)	10.79 \pm 1.85	12.39 \pm 2.05**	9.14 \pm 0.55	10.19 \pm 0.66*
PVR (mmHg/mL per min per 100 g)	1.94 \pm 0.20	2.00 \pm 0.21*	2.53 \pm 0.18	2.64 \pm 0.21*

Data are the mean \pm SEM. * $P < 0.05$, ** $P < 0.01$ compared with pre-N^G-nitro-L-arginine methyl ester (L-NAME).

MPAP, mean pulmonary arterial pressure; MABP, mean arterial blood pressure; CO, cardiac output; HR, heart rate; SVR, systemic vascular resistance; PVR, pulmonary vascular resistance.

not alter the acute hypoxic response for any of the variables recorded in either N or CH rats (Fig. 1a,b).

Cardiovascular responses to the i.v. administration of L-NAME (50 mg/kg, i.v.) were also recorded. In N rats, a bolus i.v. dose of L-NAME provoked robust systemic vasoconstriction ($123 \pm 20\%$ increase in SVR; $P < 0.001$), as well as, to a lesser extent, pulmonary vasoconstriction ($80 \pm 10\%$ increase in PVR; $P < 0.01$). The baroreflex decrease in HR and CO (NS; see baseline data in Fig. 1a,b) meant that the changes in vascular resistance were accompanied by smaller, but still significant, increases in MABP ($42 \pm 18\%$ increase in MABP; $P < 0.001$) and MPAP ($13 \pm 9\%$ increase in MPAP; NS) in N rats. After 2 weeks of chronic hypoxia, L-NAME (i.v.) had a similar effect on the systemic vasculature and caused a similar depression of HR (NS) and CO ($P < 0.001$), but it had a more pronounced effect on the pulmonary vasculature ($24 \pm 5\%$ increase in MPAP (NS); $116 \pm 18\%$ increase in PVR ($P < 0.01$)).

Treatment of N rats with L-NAME (i.v.) exacerbated the reduction in MABP and SVR in response to acute hypoxia and accentuated the increase in MPAP and PVR (Fig. 1a,b). Despite a depression in baseline values for CO and HR, i.v. administration of L-NAME did not change the transient responses to hypoxia. In CH rats, the transient MABP and SVR responses to acute hypoxia were elevated by L-NAME (i.v.). In addition, L-NAME restored the potent MPAP (and PVR) response to acute hypoxia (observed in N rats), which had been absent prior to L-NAME treatment (Fig. 1a,b).

Administration of SIN-1

Following a single bolus i.c.v. injection of SIN-1 (100 μ g) in N rats, baseline MPAP and PVR were not significantly altered. However, MABP declined slowly before stabilizing $38 \pm 7\%$ below the pre-SIN-1 baseline (Table 3). Preliminary studies

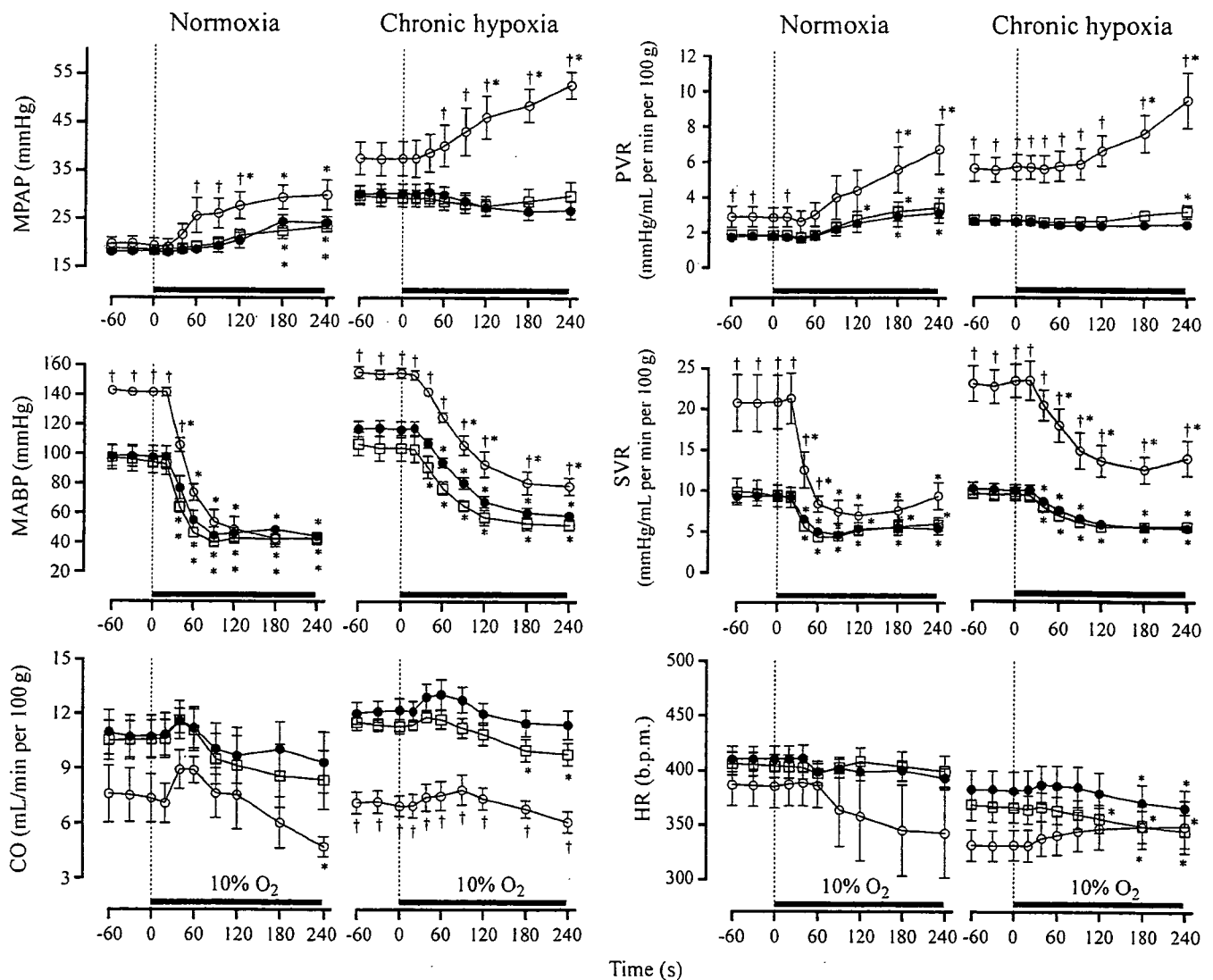


Fig. 1 Mean pulmonary arterial pressure (MPAP), mean arterial blood pressure (MABP), cardiac output (CO), pulmonary vascular resistance (PVR), systemic vascular resistance (SVR) and heart rate (HR) responses to acute hypoxia (10% O₂ for 4 min) in normoxic (N) rats ($n = 7$) and chronic hypoxic (CH) rats ($n = 5$), before (●) and after the administration of *N*^G-nitro-L-arginine methyl ester (L-NAME; □, 150 μ g in 10 μ L, i.c.v.; ◇, 50 mg/kg, i.v.). * $P < 0.05$ compared with pre-acute hypoxia values; † $P < 0.05$ compared with L-NAME values.

showed that once cardiovascular variables stabilized following the initial response to SIN-1, variables did not change for at least another 20 min. The fall in MABP was primarily attributed to vasodilatation ($29 \pm 7\%$ decrease in SVR; $P < 0.05$). In CH rats, SIN-1 (i.c.v.) did not alter PVR, but it did decrease MPAP by $21 \pm 3\%$ ($P < 0.01$) owing to a $22 \pm 5\%$ decrease in CO ($P < 0.05$). Sydnominine-1 provoked a larger decrease in CO in CH rats ($22 \pm 5\%$ decrease; $P < 0.05$), so that the fall in MABP was also greater in CH rats ($46 \pm 3\%$ decrease), because the decline in SVR was similar for N rats and CH rats (27 ± 7 and 29% decrease in SVR, respectively).

In N rats, the CO response to acute hypoxia was depressed by SIN-1 so that, even though the MPAP response appeared to be unchanged (Fig. 2a), the PVR response to hypoxia was accentuated by SIN-1 (64 ± 24 and $127 \pm 26\%$ increase, respectively; Fig. 2b). Sydnominine-1 reduced the magnitude of the MABP and SVR responses to hypoxia, although the absolute MABP (and SVR)

values during hypoxia before and after SIN-1 were similar. In addition, SIN-1 abolished the small hypoxia-induced decline in HR observed prior to SIN-1 administration.

In CH rats, SIN-1 restored the pulmonary vasoconstriction in response to acute hypoxia. This was evident by a $33 \pm 5\%$ increase in MPAP (cf. a 3% increase for control) and a $90 \pm 11\%$ increase in PVR (cf. a 20% increase for control). The effect of SIN-1 on the MABP, SVR, CO and HR responses to acute hypoxia were similar for N and CH rats (Fig. 2a,b).

DISCUSSION

To date, this is the first study to investigate the central role of NO in: (i) modulating MPAP in the normal and hypertensive state; and (ii) acute HPV. The primary findings of the present study show that, in both N and CH rats, the acute central inhibition of NOS does not appear to modulate baseline MPAP or pulmonary vascular

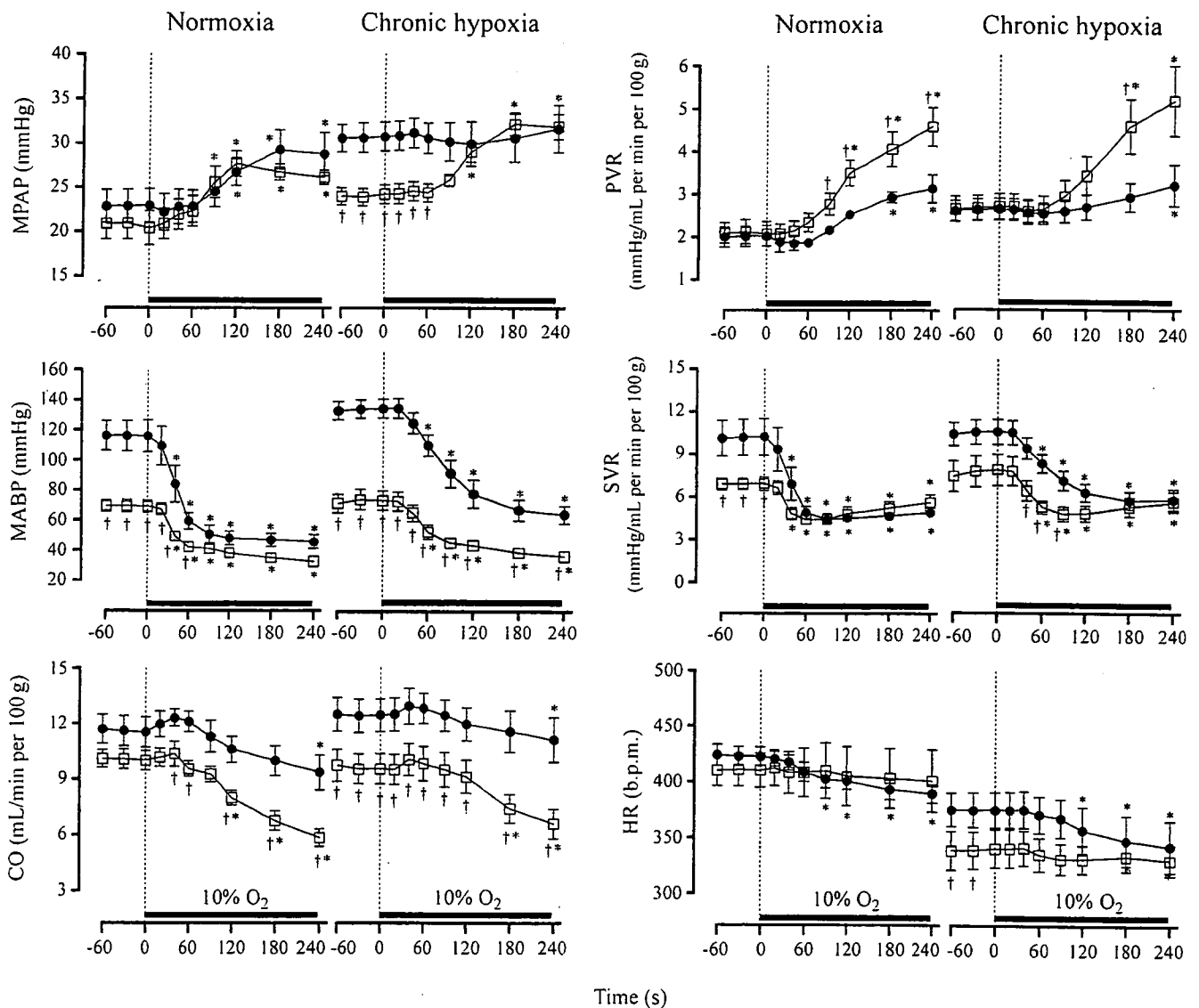


Fig. 2 Effect of i.c.v. sydnominine-1 (SIN-1) on mean pulmonary arterial pressure (MPAP), mean arterial blood pressure (MABP), cardiac output (CO), pulmonary vascular resistance (PVR), systemic vascular resistance (SVR) and heart rate (HR) responses to acute hypoxia (10% O₂ for 4 min) in normoxic (N) rats ($n = 5$) and chronic hypoxic (CH) rats ($n = 6$). (●), control (artificial cerebrospinal fluid); (□), SIN-1 (100 µg in 10 µL). * $P < 0.05$ compared with pre-acute hypoxia values; † $P < 0.05$ compared with SIN-1-values.

Table 3 Steady state responses to intracerebroventricular syndnonimine-1 (100 µg in 10 µL) in normoxic rats (*n* = 5) and chronic-hypoxic rats (*n* = 6)

	Normoxia		Chronic hypoxia	
	Control	SIN-1	SIN-1	Control
MPAP (mmHg)	22.9 ± 1.7	20.8 ± 1.8	30.6 ± 1.6	24.1 ± 1.0*
MABP (mmHg)	116 ± 10	69 ± 4*	122 ± 6	67 ± 6**
CO (mL/min per 100 g)	11.64 ± 0.81	10.08 ± 0.51	12.46 ± 0.89	9.63 ± 0.81*
HR (b.p.m.)	423 ± 9	410 ± 15	375 ± 16	339 ± 17**
SVR (mmHg/mL per min per 100 g)	10.20 ± 1.28	6.93 ± 0.42 [‡]	10.07 ± 0.82	7.36 ± 1.06*
PVR (mmHg/mL per min per 100 g)	2.02 ± 0.23	2.10 ± 0.27	2.54 ± 0.24	2.58 ± 0.28

Data are the mean ± SEM. **P* < 0.05, ***P* < 0.01 compared with control values.

SIN-1, syndnonimine-1; MPAP, mean pulmonary arterial pressure; MABP, mean arterial blood pressure; CO, cardiac output; HR, heart rate; SVR, systemic vascular resistance; PVR, pulmonary vascular resistance.

reactivity to acute hypoxia. However, exogenous NO reduces baseline MPAP in CH rats, primarily by reducing CO, and enhances the HPV.

We demonstrated that exposure to 12% O₂ for 2 weeks induced pulmonary arterial hypertension, which concurs with numerous reports in the literature regarding the effects of CH on the pulmonary vasculature.^{6,29,30} Compared with the pulmonary vasculature, the systemic vasculature seems to be less affected by CH. We did not observe any difference in MABP between N and CH rats, which is similar to some reports.^{30,31} In contrast, Huang *et al.*⁶ did note an increase in MABP after 2 weeks of CH, although they described the increase in MABP as mild compared with the increase in MPAP.

The mechanisms responsible for the development of pulmonary hypertension remain poorly understood. Although a reduction in the local release of NO from the pulmonary endothelium has been implicated,^{5,8,32} Hampl *et al.*³⁰ reported that chronic inhibition of NOS did not increase MPAP, indicating that factors other than, or in addition to, a decrease in pulmonary NOS activity were responsible for the development of pulmonary hypertension. Furthermore, Weissmann *et al.*²⁷ investigated the role of pulmonary NO in the acute HPV response and concluded that attenuation of the acute HPV by chronic hypoxia preceded the development of pulmonary hypertension and was independent of the pulmonary endothelial NO system. Therefore, we hypothesized that disruption of the central NO pathways may contribute, at least in part, to the pathogenesis of pulmonary hypertension during chronic hypoxia.

Our results indicate that, using L-NAME, central NO has a minimal role, if any, in modulating tonic pulmonary vascular tone in the normal and hypertensive state. However, we cannot rule out the possibility that the dose of L-NAME selected in the present study did not completely inhibit NOS within the cardiovascular control centres. Preliminary experiments indicated that when L-NAME is injected i.v., doses above 150 µg had small direct systemic effects (similar preliminary experiments were conducted to determine the dose of SIN-1 with which to inject i.c.v. that did not directly alter pulmonary vasculature when injected i.v.). Therefore, because L-NAME can cross the blood-brain barrier,³³ we avoided higher doses of L-NAME that could have potentially directly modulated pulmonary vascular tone. Furthermore, a study by Nurminen *et al.*³⁴ reported that 30 µg L-NAME, i.c.v., provoked a significant increase in ABP that lasted for 10 min. Therefore, we were confident that a dose of 150 µg L-NAME would induce sufficient central NOS inhibition.

Although we found that L-NAME did not alter the acute HPV, we cannot exclude the possibility that the central actions of

L-NAME had fully subsided before testing acute hypoxia. However, preliminary experiments (data not shown) indicated that, even when L-NAME was administered immediately before the acute hypoxic test, the cardiovascular responses to acute hypoxia were not different to the responses prior to L-NAME. Alternatively, acute hypoxia is known to be a powerful activator of sympathetic nerve activity.³⁵ Because it has been well documented that the central administration of L-NAME increases sympathetic activity,^{36,37} it may be possible that, in the present study, L-NAME did not alter the HVR because sympathetic activity was already elevated by the acute hypoxic stimulus.

Although central L-NAME did not alter pulmonary vasculature tone, the intravenous administration of L-NAME did cause a small increase in PVR in N rats, which was accentuated after chronic hypoxia. Furthermore, the acute HVR was accentuated by L-NAME (i.v.) in both N and CH rats. Several studies have indicated that local endothelial NO has a limited role, if any, in the tonic modulation of MPAP,^{6,38} although Huang *et al.*⁶ indicated that local NO: (i) was more important in modulating pulmonary vasculature after chronic hypoxia; and (ii) was essential for maintaining low pulmonary resistance during acute hypoxia.

In comparison, the magnitude of the systemic vasoconstrictive response to L-NAME (i.v.) was substantially larger than that of the pulmonary vasculature. In agreement, several studies have indicated that local inhibition of NOS has an insignificant effect on tonic modulation of the pulmonary vasculature, but it is critical in modulating the systemic vasculature.^{6,30,38}

It has been well documented that central inhibition of NO increases MABP^{34,39,40} by increasing sympathetic nerve activity.^{36,37} We also reported that i.c.v. L-NAME provoked a significant increase in MABP, although one of the limitations of the present study is that we did not measure sympathetic activity. However, we found that the provoked increase in MABP by i.c.v. L-NAME in the normoxic rat was not accompanied by a baroreflex decrease in HR, which occurs when L-NAME is injected intravenously. Nurminen *et al.*³⁴ also reported that i.c.v. L-NAME caused a paradoxical increase in HR and, thus, concluded that the increase in HR was indirect evidence that L-NAME provoked an increase in sympathetic activity.

With regards to the pulmonary vasculature, an increase in sympathetic activity can cause either vasoconstriction (α -adreno-receptor mediated) or vasodilation (β -adreno-receptor mediated), depending on the initial pulmonary vascular tone.^{41,42} Therefore, assuming that i.c.v. L-NAME did increase pulmonary sympathetic activity, it is possible that we were unable to detect any change

in MPAP because of the potential opposing effects of α - and β -adrenoceptor activation within the pulmonary vasculature.

In the present study, as well as in other studies, the central administration of NO donors has been shown to reduce MABP.^{25,43} Nurminen and Vapaatalo⁴⁴ also showed that certain NO-releasing substances, such as nitroprusside, reduced MABP, although they also mentioned that the central administration of SIN-1 (approximately 600 $\mu\text{g}/\text{kg}$) increased MABP.

At high doses, SIN-1 can cogenerate NO and superoxide anions.^{45,46} Furthermore, an increase in the central generation of superoxide anions has been reported to increase sympathetic activity and, consequently, ABP.⁴⁷ Therefore, the increase in MABP in the study of Nurminen and Vapaatalo⁴⁴ may be attributed to the formation of superoxide anions. At low doses, the superoxide-associated effects of SIN-1 are significantly outweighed by the actions of NO.⁴⁵ Therefore, because the present study used a comparatively low dose of SIN-1 (100 μg), we interpret the decrease in MABP to indicate that, at this dose, SIN-1 was acting solely as an NO donor.

The decrease in MABP following the central administration of exogenous NO has been attributed to a decrease in sympathetic activity.^{40,48} To date, the present study is the first to investigate the effects of a central NO donor on MPAP. The important finding of the present study is that exogenous NO did not directly alter baseline pulmonary vascular tone (i.e. PVR was not altered), but it did enhance (in N rats) or restore (in CH rats) the acute HPV response. These results support the idea that central NO has little influence on the tonic modulation of pulmonary vascular tone, although it enhances the acute HPV.

Although we cannot confirm the underlying mechanisms responsible for these observations, it is possible that SIN-1 did reduce sympathetic activity in the rats in the present study, subsequently enhancing the HPV. Shirai *et al.*⁴⁹ demonstrated that β -adrenoceptor blockade had only a minor effect on baseline pulmonary vascular tone in normoxia, but it significantly accentuated the acute HPV (α -adrenoceptor blockade had no effect on the magnitude of the HPV). This observation may explain the reason as to why central SIN-1 did not affect baseline PVR but accentuated the HPV in the present study. Although PVR was not affected, central SIN-1 did reduce MPAP in the present study (significantly in CH rats), solely due to a reduction in CO. This, too, may be due to a reduction in β -adrenoceptor activity, because β -adrenoceptor attenuation has been reported to significantly reduce CO.^{50,51}

The mechanism(s) responsible for the attenuation of the HPV after chronic hypoxia remain poorly understood. However, it is possible to speculate that β -adrenoceptor upregulation may be one contributing factor because previous studies have shown that chronic hypoxia significantly increases β -adrenoceptor numbers within the lung.^{52,53} Changes in β -adrenoceptor availability during chronic hypoxia could potentially limit the development of pulmonary hypertension and, therefore, be physiologically beneficial; an important area that warrants further research.

In summary, we have shown that central NO has a limited role in modulating tonic MPAP in the normal and hypertensive states. However, exogenous NO enhanced the acute HPV, although central NO inhibition had no effect on the acute HPV. Whether central NO acts to inhibit β -adrenoceptor-mediated vasodilation of the acute HPV is another area that warrants further investigation. The present study used an anaesthetized preparation to investigate the

modulation of MPAP in normoxia and after chronic hypoxia. We did not, however, address any potential changes in the control of MPAP during the development of pulmonary hypertension. Hampl and Herget³⁸ indicated that, during the development of pulmonary hypertension, NO was essential in preventing pulmonary hypertension in the early stages, but became insignificant in the latter stages owing to endothelial dysfunction. Therefore, we will subsequently develop a conscious, chronically cannulated rat model to monitor the development of pulmonary hypertension during the chronic central inhibition/infusion of NO.

ACKNOWLEDGEMENT

The authors are very grateful for the aid and support provided by the Japan Society for the Promotion of Science (JSPS).

REFERENCES

1. Archer S, Rich S. Primary pulmonary hypertension: A vascular biology and translational research 'work in progress'. *Circulation* 2000; **102**: 2781–91.
2. Mandegar M, Yuan JX. Role of K^+ channels in pulmonary hypertension. *Vasc. Pharmacol.* 2002; **38**: 25–33.
3. Barbera JA, Peinado VI, Santos S. Pulmonary hypertension in COPD: Old and new concepts. *Monaldi Arch. Chest Dis.* 2000; **55**: 445–9.
4. Voelkel NF, Tudor RM. Hypoxia-induced pulmonary vascular remodeling: A model for what human disease? *J. Clin. Invest.* 2000; **106**: 733–8.
5. Fike CD, Kaplowitz MR, Thomas CJ, Nelin LD. Chronic hypoxia decreases nitric oxide production and endothelial nitric oxide synthase in newborn pig lungs. *Am. J. Physiol.* 1998; **274**: L517–26.
6. Huang KL, Wu CP, Kang BH, Lin YC. Chronic hypoxia attenuates nitric oxide-dependent hemodynamic responses to acute hypoxia. *J. Biomed. Sci.* 2002; **9**: 206–12.
7. Cornwell TL, Arnold E, Boerth NJ, Lincoln TM. Inhibition of smooth muscle cell growth by nitric oxide and activation of cAMP-dependent protein kinase by cGMP. *Am. J. Physiol.* 1994; **267**: C1405–13.
8. Le Cras TD, McMurtry IF. Nitric oxide production in the hypoxic lung. *Am. J. Physiol. Lung Cell. Mol. Physiol.* 2001; **280**: L575–82.
9. Sato J, Nair K, Hiddinga J *et al.* eNOS gene transfer to vascular smooth muscle cells inhibits cell proliferation via upregulation of p27 and p21 and not apoptosis. *Cardiovasc. Res.* 2000; **47**: 697–706.
10. Palmer RM, Rees DD, Ashton DS, Moncada S. L-Arginine is the physiological precursor for the formation of nitric oxide in endothelium-dependent relaxation. *Biochem. Biophys. Res. Commun.* 1988; **153**: 1251–6.
11. Fagan KA, Fouty BW, Tyler RC *et al.* The pulmonary circulation of homozygous or heterozygous eNOS-null mice is hyperresponsive to mild hypoxia. *J. Clin. Invest.* 1999; **103**: 291–9.
12. Steudel W, Ichinose F, Huang PL *et al.* Pulmonary vasoconstriction and hypertension in mice with targeted disruption of the endothelial nitric oxide synthase (NOS 3) gene. *Circ. Res.* 1997; **81**: 34–41.
13. Steudel W, Scherrer-Crosbie M, Bloch KD *et al.* Sustained pulmonary hypertension and right ventricular hypertrophy after chronic hypoxia in mice with congenital deficiency of nitric oxide synthase 3. *J. Clin. Invest.* 1998; **101**: 2468–77.
14. Ozaki M, Kawashima S, Yamashita T *et al.* Reduced hypoxic pulmonary vascular remodeling by nitric oxide from the endothelium. *Hypertension* 2001; **37**: 322–7.
15. Sato K, Rodman DM, McMurtry IF. Hypoxia inhibits increased ET_B receptor-mediated NO synthesis in hypertensive rat lungs. *Am. J. Physiol.* 1999; **276**: L571–81.
16. Xue C, Rengasamy A, Le Cras TD, Koberna PA, Dailey GC, Johns RA. Distribution of NOS in normoxic vs. Hypoxic rat lung:

- Upregulation of NOS by chronic hypoxia. *Am. J. Physiol.* 1994; **267**: L667–78.
17. Shirai M, Pearson JT, Shimouchi A *et al.* Changes in functional and histological distributions of nitric oxide synthase caused by chronic hypoxia in rat small pulmonary arteries. *Br. J. Pharmacol.* 2003; **139**: 899–910.
 18. Le Cras TD, Xue C, Rengasamy A, Johns RA. Chronic hypoxia upregulates endothelial and inducible NO synthase gene and protein expression in rat lung. *Am. J. Physiol.* 1996; **270**: L164–70.
 19. Matsumura K, Tsuchihashi T, Kagiya S, Abe I, Fujishima M. Role of nitric oxide in the nucleus of the solitary tract of rats. *Brain Res.* 1998; **798**: 232–8.
 20. Zanzinger J, Czachurski J, Sellar H. Inhibition of basal and reflex-mediated sympathetic activity in the RVLM by nitric oxide. *Am. J. Physiol.* 1995; **268**: R958–62.
 21. Ohta A, Takagi H, Matsui T, Hamai Y, Iida S, Esumi H. Localization of nitric oxide synthase-immunoreactive neurons in the solitary nucleus and ventrolateral medulla oblongata of the rat: Their relation to catecholaminergic neurons. *Neurosci. Lett.* 1993; **158**: 33–5.
 22. Garthwaite J, Boulton CL. Nitric oxide signaling in the central nervous system. *Annu. Rev. Physiol.* 1995; **57**: 683–706.
 23. Patel KP, Li YF, Hirooka Y. Role of nitric oxide in central sympathetic outflow. *Exp. Biol. Med.* 2001; **226**: 814–24.
 24. Hironaga K, Hirooka Y, Matsuo I *et al.* Role of endogenous nitric oxide in the brain stem on the rapid adaptation of baroreflex. *Hypertension* 1998; **31**: 27–31.
 25. Nishimura M, Takahashi H, Nanbu A, Sakamoto M, Yoshimura M. Cardiovascular regulation by L-arginine in the brain of rats: Role of the brain renin-angiotensin system and nitric oxide. *Am. J. Hypertens.* 1997; **10**: 389–96.
 26. Clini E, Ambrosino N. Nitric oxide and pulmonary circulation. *Med. Sci. Monit.* 2002; **8**: RA178–82.
 27. Weissmann N, Nollen M, Gerigk B *et al.* Downregulation of hypoxic vasoconstriction by chronic hypoxia in rabbits: Effects of nitric oxide. *Am. J. Physiol. Heart Circ. Physiol.* 2003; **284**: H931–8.
 28. Paxinos G, Watson C. *The Brain in Stereotaxic Coordinates*, 4th edn. Academic Press, San Diego, CA. 1998.
 29. Ao Q, Huang L, Zhu P, Xiong M, Wang D. Inhibition of expression of hypoxia-inducible factor-1 α mRNA by nitric oxide in hypoxic pulmonary hypertension rats. *J. Huazhong Univ. Sci. Technol. Med. Sci.* 2004; **24**: 5–8.
 30. Hampf V, Archer SL, Nelson DP, Weir EK. Chronic EDRF inhibition and hypoxia: Effects on pulmonary circulation and systemic blood pressure. *J. Appl. Physiol.* 1993; **75**: 1748–57.
 31. Coney AM, Bishay M, Marshall JM. Influence of endogenous nitric oxide on sympathetic vasoconstriction in normoxia, acute and chronic systemic hypoxia in the rat. *J. Physiol.* 2004; **555**: 793–804.
 32. Adnot S, Raffestin B, Eddahibi S, Braquet P, Chabrie PE. Loss of endothelium-dependent relaxant activity in the pulmonary circulation of rats exposed to chronic hypoxia. *J. Clin. Invest.* 1991; **87**: 155–62.
 33. Bansinath M, Arbabha B, Turndorf H, Garg UC. Chronic administration of a nitric oxide synthase inhibitor N-nitro-L-arginine, and drug-induced increase in cerebellar cyclic GMP *in vivo*. *Neurochem. Res.* 1993; **18**: 1063–6.
 34. Nurminen ML, Ylikorkala A, Vapaatalo H. Central inhibition of nitric oxide synthesis increases blood pressure and heart rate in anesthetized rats. *Methods Fundam. Exp. Clin. Pharmacol.* 1997; **19**: 35–41.
 35. Fletcher EC. Invited review: Physiological consequences of intermittent hypoxia: Systemic blood pressure. *J. Appl. Physiol.* 2001; **90**: 1600–5.
 36. Harada S, Tokunaga S, Momohara M *et al.* Inhibition of nitric oxide formation in the nucleus tractus solitarius increases renal sympathetic nerve activity in rabbits. *Circ. Res.* 1993; **72**: 511–16.
 37. Zanzinger J, Czachurski J, Sellar H. Nitric oxide in the ventrolateral medulla regulates sympathetic responses to systemic hypoxia in pigs. *Am. J. Physiol.* 1998; **275**: R33–9.
 38. Hampf V, Herget J. Role of nitric oxide in the pathogenesis of chronic pulmonary hypertension. *Physiol. Rev.* 2000; **80**: 1337–72.
 39. Choi KC, Jung M, Lee JU, Kim SW, Kim NH, Kang YJ. Attenuated central pressor response to nitric oxide synthesis inhibition in chronic renal failure rats. *Korean J. Intern. Med.* 1997; **12**: 58–61.
 40. Togashi H, Sakuma I, Yoshioka M *et al.* A central nervous system action of nitric oxide in blood pressure regulation. *J. Pharmacol. Exp. Ther.* 1992; **262**: 343–7.
 41. Shirai M, Shindo T, Shimouchi A, Ninomiya I. Diameter and flow velocity changes of feline small pulmonary vessels in response to sympathetic nerve stimulation. *Pflügers Arch.* 1994; **429**: 267–73.
 42. Shirai M, Matsukawa K, Nishiura N, Kawaguchi AT, Ninomiya I. Changes in efferent pulmonary sympathetic nerve activity during systemic hypoxia in anesthetized cats. *Am. J. Physiol.* 1995; **269**: R1404–9.
 43. Matsumura K, Abe I, Tsuchihashi T, Fujishima M. Central nitric oxide attenuates the baroreceptor reflex in conscious rabbits. *Am. J. Physiol.* 1998; **274**: R1142–9.
 44. Nurminen ML, Vapaatalo H. Effect of intracerebroventricular and intravenous administration of nitric oxide donors on blood pressure and heart rate in anaesthetized rats. *Br. J. Pharmacol.* 1996; **119**: 1422–6.
 45. Stopper H, Moller M, Bommel HM, Schmidt HH. Cytotoxic versus genotoxic effects of nitric oxide (NO). *Toxicol. Lett.* 1999; **106**: 59–67.
 46. Megson IL, Webb DJ. Nitric oxide donor drugs: Current status and future trends. *Expert Opin. Investig. Drugs* 2002; **11**: 587–601.
 47. Gao L, Wang W, Li YL *et al.* Superoxide mediates sympathoexcitation in heart failure: Roles of angiotensin II and NAD(P)H oxidase. *Circ. Res.* 2004; **95**: 937–44.
 48. Shapoval LN, Sagach VF, Pobegailo LS. Nitric oxide influences ventrolateral medullary mechanisms of vasomotor control in the cat. *Neurosci. Lett.* 1991; **132**: 47–50.
 49. Shirai M, Shindo T, Ninomiya I. β -Adrenergic mechanisms attenuated hypoxic pulmonary vasoconstriction during systemic hypoxia in cats. *Am. J. Physiol.* 1994; **266**: H1777–85.
 50. Kontos HA, Lower RR. Role of beta-adrenergic receptors in the circulatory response to hypoxia. *Am. J. Physiol.* 1969; **217**: 756–63.
 51. Chiong MA, Hatcher JD. The sympathoadrenergic system in the cardiovascular response to hypoxia in the dog. *Can. J. Physiol. Pharmacol.* 1972; **50**: 674–83.
 52. Birnkrant DJ, Davis PB, Ernsberger P. Visualization of high- and low-affinity beta-adrenergic receptors in rat lung: Upregulation by chronic hypoxia. *Am. J. Physiol.* 1993; **265**: L389–94.
 53. Winter RJ, Dickinson KE, Rudd RM, Sever PS. Tissue specific modulation of beta-adrenoceptor number in rats with chronic hypoxia with an attenuated response to down-regulation by salbutamol. *Clin. Sci.* 1986; **70**: 159–65.

PRECLINICAL RESEARCH

Beneficial Effect of Hydroxyfasudil, a Specific Rho-Kinase Inhibitor, on Ischemia/Reperfusion Injury in Canine Coronary Microcirculation In Vivo

Toyotaka Yada, MD, PHD,* Hiroaki Shimokawa, MD, PHD,† Osamu Hiramatsu, PHD,* Tatsuya Kajita, MD, PHD,* Fumiuyuki Shigeto, MD, PHD,* Etsuro Tanaka, MD, PHD,‡ Yoshiro Shinozaki, BS,§ Hidezo Mori, MD, PHD,|| Takahiko Kiyooka, MD,# Masashi Katsura, PHD,¶ Seitaro Ohkuma, MD, PHD,¶ Masami Goto, MD, PHD,* Yasuo Ogasawara, PHD,* Fumihiko Kajiya, MD, PHD#

Kurashiki, Fukuoka, Tokyo, Isehara, Suita, and Okayama, Japan

OBJECTIVES	We examined whether hydroxyfasudil, a specific Rho-kinase inhibitor, exerts cardioprotective effect on coronary ischemia/reperfusion (I/R) injury and, if so, whether nitric oxide (NO) is involved.
BACKGROUND	Recent studies have demonstrated that Rho-kinase is substantially involved in the pathogenesis of cardiovascular diseases; however, it remains to be examined whether it is also involved in ischemia/reperfusion (I/R) injury.
METHODS	Canine subepicardial small arteries (SA, $\geq 100 \mu\text{m}$) and arterioles (A, $< 100 \mu\text{m}$) were observed by a charge-coupled device intravital microscope during I/R. Coronary vascular responses to endothelium-dependent (acetylcholine, intracoronary [IC]) and -independent (papaverine, IC) vasodilators were examined after I/R under the following four conditions: control (n = 7), NO synthase inhibitor alone (N ^G -monomethyl-L-arginine [L-NMMA], IC, n = 4), hydroxyfasudil alone (IC, n = 7), and hydroxyfasudil plus L-NMMA (n = 7).
RESULTS	Hydroxyfasudil significantly attenuated serotonin (IC)-induced vasoconstriction of SA ($-7 \pm 1\%$ vs. $2 \pm 1\%$, $p < 0.01$). Coronary I/R significantly impaired coronary vasodilation to acetylcholine after I/R (SA, $p < 0.05$; and A, $p < 0.01$ vs. before I/R) and L-NMMA further reduced the vasodilation, whereas hydroxyfasudil completely preserved the responses. The vasoconstriction by L-NMMA after I/R was significantly improved by hydroxyfasudil in both-sized arteries (both $p < 0.01$). Expression of endothelial nitric oxide synthase (eNOS) protein in the ischemic endocardium of left anterior descending coronary artery area (as determined by Western blotting) significantly decreased ($79 \pm 4\%$) compared with the nonischemic endocardium of LCX area ($100 \pm 7\%$), which was improved by hydroxyfasudil ($105 \pm 6\%$, $p < 0.01$). Hydroxyfasudil significantly reduced myocardial infarct size, and hydroxyfasudil with L-NMMA also reduced the infarct size compared with L-NMMA alone.
CONCLUSIONS	Hydroxyfasudil exerts cardioprotective effects on coronary I/R injury in vivo, in which NO-mediated mechanism may be involved through preservation of eNOS expression. (J Am Coll Cardiol 2005;45:599-607) © 2005 by the American College of Cardiology Foundation

Ischemia-reperfusion (I/R) injury attenuates endothelium-dependent dilation of large coronary arteries both in vitro (1,2) and in vivo (3,4). Endothelial dysfunction causes adverse outcome in the coronary circulation (5). Reperfu-

sion injury is caused by direct myocardial injury through coronary vasospasm, free radicals, and inflammatory responses (6,7). Furthermore, local coronary vasoconstrictions in response to vasoconstrictors (e.g., serotonin) are enhanced (8,9). However, the mechanism of I/R-induced vascular injury remains to be clarified.

Recent studies have demonstrated that Rho-kinase, an effector of the small guanosine triphosphatase Rho, is substantially involved in the pathogenesis of cardiovascular diseases (10). Shimokawa et al. (10,11) have recently found that hydroxyfasudil is a potent and specific inhibitor of Rho-kinase and markedly inhibits coronary hypercontraction and macrophage migration. They also demonstrated that intracoronary serotonin induces coronary hypercontractions at the inflammatory coronary lesions both in vitro and in vivo, in which up-regulated Rho-kinase is substantially

From the *Department of Medical Engineering and Systems Cardiology, Kawasaki Medical School, Kurashiki, Japan; †Department of Cardiovascular Medicine, Kyushu University Graduate School of Medical Sciences, Fukuoka, Japan; ‡Faculty of Applied Bioscience, Tokyo University of Agriculture, Tokyo, Japan; §Department of Physiology, Tokai University School of Medicine, Isehara, Japan; ||Department of Cardiac Physiology, National Cardiovascular Center Research Institute, Suita, Japan; ¶Department of Pharmacology, Kawasaki Medical School, Kurashiki, Japan; and #Department of Cardiovascular Physiology, Okayama University Graduate School of Medicine and Dentistry, Okayama, Japan. This work was supported in part by grants from the Japanese Ministry of Education, Science, Sports, Culture, and Technology, Tokyo, Japan (Nos. 13307024, 13557068, 14657178, and 16300164); and the Program for Promotion of Fundamental Studies in Health Sciences of the Organization for Pharmaceutical Safety and Research of Japan.

Manuscript received September 2, 2004; revised manuscript received October 1, 2004; accepted October 18, 2004.

Abbreviations and Acronyms

I/R = ischemia-reperfusion
LAD = left anterior descending coronary artery
LCX = left circumflex artery
NO = nitric oxide

involved (12). Recent studies demonstrated that endothelial expression and activity of Rho-kinase are enhanced by hypoxia, with a resultant down-regulation of endothelial nitric oxide synthase (eNOS) expression and reduced nitric oxide (NO) production (13), and that Rho-kinase is also involved in a canine model of cerebral infarction associated with superoxide production and neutrophil infiltration (14).

It is conceivable that Rho-kinase is involved in the mechanisms of I/R injury associated with reduced endothelial NO production. In this study, we thus examined whether hydroxyfasudil exerts protective effect on coronary I/R injury *in vivo* and, if so, whether NO is involved.

METHODS

Animal preparation. This study conformed to the Guideline on Animal Experiments of Kawasaki Medical School and the Guide for the Care and Use of Laboratory Animals published by the U.S. National Institutes of Health.

Mongrel dogs (15 to 25 kg, $n = 31$) of either gender were anesthetized with morphine (3 mg/kg, intramuscular) and sodium pentobarbital (25 mg/kg, intravenous). After intubation, each animal was ventilated with a high-frequency jet ventilator (model VS600, IDC, Pittsburgh, Pennsylvania) with room air supplemented by 100% oxygen. Aortic pressure and left ventricular pressure were continuously monitored with an 8-F pigtail double manometer catheter (SPC-784A, Millar, Texas). The proximal portion of the left anterior descending coronary artery (LAD) was isolated and a transonic flow probe (T206, Transonic Systems, Ithaca, New York) was placed around the vessel.

Needle-probe intravital microscope. The needle-probe (4.5 mm in diameter, VMS 1210, Nihon Kohden, Tokyo, Japan) contains a gradient index lens (with a magnification of 200) surrounded by light guide fibers and a double lumen sheath. A doughnut-shaped balloon on the tip avoids direct compression of the vessels by the needle tip (15).

Measurements of coronary diameters. We placed the needle probe gently on subepicardial microvessels. When a clear vascular image was obtained, end-diastolic vascular images were taken with 30 pictures/s (15).

Measurements of regional myocardial blood flow. Regional myocardial blood flow was determined by the non-radioactive microsphere (Sekisui Plastic Co, Ltd, Tokyo, Japan) technique, as previously described in detail (16). Briefly, 1 ml of the microspheres suspension (2 to 4×10^6 spheres) was injected into the left atrium 85 min after the onset of coronary occlusion. Just before microsphere administration, a reference blood flow sample was drawn from the

femoral artery at a constant rate of 8 ml/min for 2 min. The X-ray fluorescence of the stable heavy elements was measured by a wavelength-dispersive spectrometer (model PW 1480, Phillips Co., Ltd., Eindhoven, the Netherlands) (16). Myocardial blood flow was calculated according to the formula: time flow = tissue counts \times (reference flow/reference counts) and was expressed in ml/g per minute (16).

Western blotting. Proteins were separated on sodium dodecyl sulfate (SDS)/polyacrylamide gel electrophoresis as previously described (17). The tissues were homogenized in a sample buffer (100 mM Tris-HCl [pH 6.8], 4% SDS, 0.2% glycerol). The tissue lysate was centrifuged and the supernatant collected. Protein concentration was quantified by a bicinchoninate (BCA) protein assay kit (Pierce Chemical, Rockford, Illinois). An aliquot of 10 μ g of protein from each sample was electrophoresed on a 7.5% SDS-polyacrylamide gel. Proteins were subsequently transferred to polyvinylidene difluoride membrane (Immobilon-P membrane, Millipore, Bedford, Massachusetts) electrophoretically (100 V for 1 h) and membranes were incubated with antibody. The antibodies used in this study were rabbit anti-phosphorylated ezrin/radixin/moesin (ERM) family, total ERM. The antibody against phosphorylated ERM recognizes human moesin (phosphorylated at Thr558), which also binds to the phosphorylated ezrin (Thr567) and radixin (Thr564). Therefore, we used the extent of phosphorylation of ERM as a marker of Rho-kinase activity. The levels of Western blot for phosphorylated ERM were normalized to those for total ERM as a control. Membranes were then incubated with a horseradish peroxidase-conjugated horse anti-rabbit immunoglobulin G antibody (1:5,000). Immunoreactivity was detected by enhanced chemiluminescence autoradiography (ECL Western blotting detection kit; Amersham Pharmacia Biotechnology, United Kingdom).

The obtained samples were washed with ice-cold Tris-HCl buffer (pH 7.4), mixed with the sample buffer (4% sodium lauryl sulfate, 12% beta-mercaptoethanol, and 20% glycerol in 100 mM Tris-HCl [pH 6.8]), sonicated (1 min), boiled (3 min), and finally centrifuged (10,000 g, 60 min, 4°C). The resultant supernatant was stored at -80°C until use. The separation of proteins was carried out according to the previous study (18), with a minor modification. The relative intensity of immunoreactive bands was quantified by Image Master 1D Elite software (Amersham Biotech, Buckinghamshire, United Kingdom), and the data were estimated as percentage of each control.

Experimental protocols. After the surgical procedure and instrumentation, at least 30 min were allowed for stabilization while hemodynamic variables were monitored. The following protocols were examined.

1. We infused graded doses of hydroxyfasudil (10, 30, and 100 μ g/kg, IC), and coronary vascular responses were

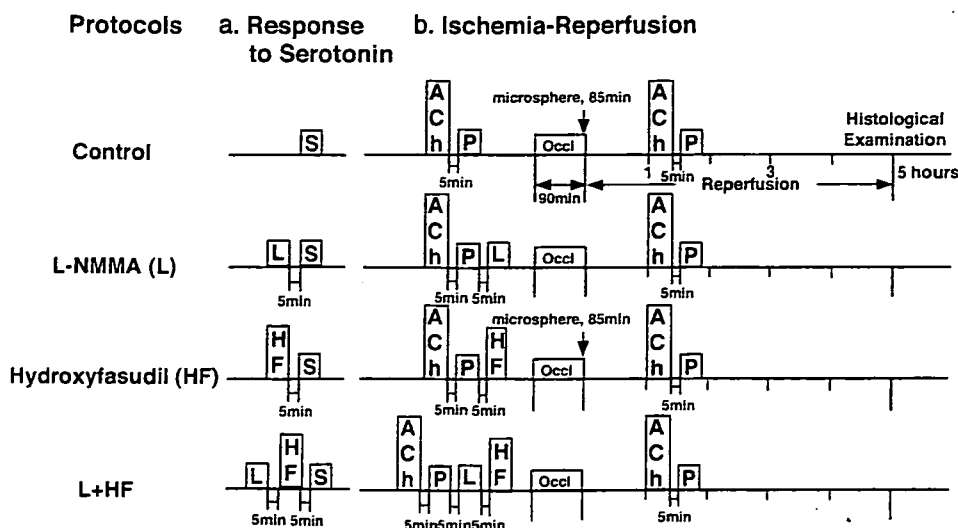


Figure 1. Experimental protocol. S = serotonin; L = L-NMMA; HF = hydroxyfasudil; Ach = acetylcholine; P = papaverine; Occl = coronary occlusion.

analyzed for 4 min by measuring end-diastolic vascular diameters and flows of the LAD.

- The arteriolar vasoconstrictor response to serotonin before and after hydroxyfasudil (100 $\mu\text{g}/\text{kg}$, IC) was examined with or without inhibition of NO synthase (L-NMMA, 2 $\mu\text{mol}/\text{min}$ for 20 min, IC) (Fig. 1). Hydroxyfasudil or L-NMMA was administered at 5 min before infusion of serotonin. The time interval between L-NMMA and hydroxyfasudil was also 5 min.
- The arteriolar vasodilator responses to endothelium-dependent (acetylcholine, 1 $\mu\text{g}/\text{kg}$ IC) and -independent (papaverine, 1 mg IC) vasodilators were examined before and after coronary I (90 min)/R (60 min) under the following four conditions separately in different animals: 1) control conditions, 2) L-NMMA alone, 3) hydroxyfasudil alone (100 $\mu\text{g}/\text{kg}$ IC), and 4) hydroxyfasudil plus L-NMMA (Fig. 1). The time interval between each treatment was also 5 min. The basal coronary diameter is before administration of acetylcholine or papaverine either

before or after I/R. Hydroxyfasudil and L-NMMA were administered at 5 min after administration of acetylcholine or papaverine. Microspheres were administered at 85 min after the onset of coronary occlusion.

- After 5 h of reperfusion, LAD and the left circumflex artery (LCX) and myocardial tissue of LAD and LCX area were obtained for Western blotting. We reoccluded the LAD and injected Evans blue dye into a systemic vein. Then myocardial slices (5 mm) were incubated in 1% 2,3,5-triphenyltetrazolium chloride (Sigma, Japan) solution to detect the infarct area. Infarct size was expressed as percentage of the infarct area that was contiguous with area at risk (19).

Drugs. We used the following drugs: hydroxyfasudil (Asahi Kasei Pharma, Tokyo, Japan), acetylcholine (Daiichi-Seiyaku, Tokyo, Japan), papaverine (Dainihon-Seiyaku, Tokyo, Japan), and N^G -methyl-L-arginine (L-

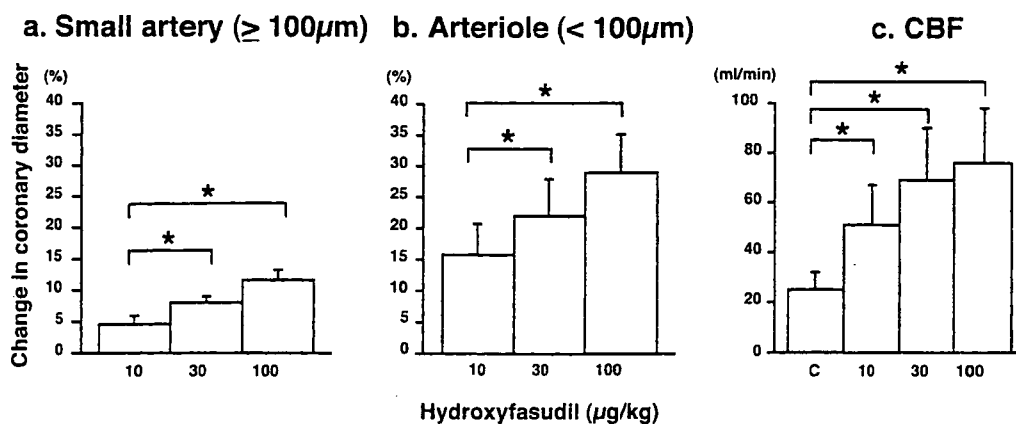


Figure 2. Coronary vasodilator effects of hydroxyfasudil in dogs in vivo. Hydroxyfasudil (10, 30, and 100 $\mu\text{g}/\text{kg}$, IC) caused coronary vasodilation, in a dose-dependent manner, under normal conditions in both small arteries (a) and arterioles (b). Number of vessels per animal used was 5/3 in small arteries and 7/4 in arterioles, respectively. Hydroxyfasudil also increased coronary blood flow (CBF) in a dose-dependent manner (c). * $p < 0.05$.